

# Neutrino generators: Foundation, Status and Future

Ulrich Mosel

Institut fuer Theoretische Physik, Universitaet Giessen, Giessen, Germany

E-mail: [mosel@physik.uni-giessen.de](mailto:mosel@physik.uni-giessen.de)

17 May 2022

**Abstract.** Neutrino generators are an essential tool needed for the extraction of neutrino mixing parameters, the mass hierarchy and a possibly CP violating phase from long-baseline experiments. In this article I first describe in quite general terms the theoretical basis and the approximations needed to get to present-days generators. I then confront present day's generators with this theoretical basis by detailed discussions of the various reaction processes. I also discuss the strengths and limitations of theoretical models used to describe semi-inclusive neutrino-nucleus reactions. As examples I then show results of the generator GiBUU for lepton semi-inclusive cross sections as well as particle spectra and discuss some features of these cross sections in terms of the various reaction components. Finally, I argue for the need for a new neutrino generator that respects our present-day knowledge of both nuclear theory and nuclear reactions and I outline some necessary requirements for such a generator.

*Keywords:* Neutrino Interactions, Neutrino Generators, Electroweak Interactions, Nuclei  
*Submitted to:* *J. Phys. G: Nucl. Phys.*

## 1. Introduction

Electron scattering on nuclei has been an active field of nuclear physics research over many decades. It has increased our knowledge about the response of a nuclear many-body system to the electromagnetic interaction [1]. At relatively low energies (10s of MeV) collective excitations of the nucleus are dominant, at higher energies (100 MeV) quasielastic reactions on individual nucleons become essential [2], at still higher energies (100s of MeV) one enters the regime of nucleon resonance excitations and finally, at the highest energies (10s of GeV), the reactions explore the Deep Inelastic Scattering (DIS) regime [3]. Originally unexpected phenomena such as 2p2h excitations [4], in-medium spectral functions [5, 6], short-range correlations [7] and spectroscopic factors [8] and the change of parton distributions inside the nucleus, as showing up in the EMC effect [9], have been explored. For all of these features not only the incoming beam energy is important, but in addition also the momentum transfer.

It is, therefore, natural to extend these studies to reactions with neutrinos where the axial coupling, typical for weak interactions, offers a new degree of freedom to explore [10]. Indeed, such studies were originally motivated by the interest in the axial response of nuclear many-body systems. In the first such studies, nearly 50 years ago, the nucleus was described as an unbound system of freely moving nucleons with their momenta determined by the Fermi-gas distribution [11, 12]. First steps beyond that simple model were studies where the nucleus was described as a bound system with a mean-field potential and excitations were treated by the Random Phase Approximation (RPA)[13, 14, 15]. More recently, even ab-initio calculations of the electroweak response of nuclei have become possible [16]. In general, neutrino-induced reactions exhibit the same characteristics as the electron-induced reactions. The same reaction subprocesses as described above also are present here. The only difference being the presence of an axial amplitude in all processes; the final state interactions are the same [17] if the incoming kinematical conditions (energy- and momentum-transfer) are identical.

Even though these two types of experiments, electron-induced and neutrino-induced ones, are so similar there is a very essential differences between them. In electron-induced the reactions the incoming beam energy is very accurately known and the momentum transfer can be measured with the help of magnetic spectrometers. Both of these observables are not available for neutrinos. Because neutrino beams are produced through the secondary decay of pion and kaons, first produced in a p+A reaction, their energies are not sharp, but smeared out over a wide range. For example, for the Deep Underground Neutrino Experiment (DUNE) [18] the energy distributions peaks at about 2 GeV, but has long tails all the way down to zero energy and up to 30 GeV. In a charged current (CC) reaction the outgoing lepton's energy and angle can be measured, but since the incoming energy is not known, also the momentum transfer is experimentally not available. This is per se a challenge for any comparison of theory with experimental results since the theory calculations have to be performed at many different energies. It also presents a challenge to theory because even lepton semi-inclusive cross sections

cannot be easily separated according to the first interaction process since the smearing of the incoming energy automatically brings with it a smearing of the energy- and momentum-transfer. For example, even at the lower energies of the T2K experiment (beam energy peak at about 0.75 GeV [19]) true quasielastic (QE) scattering on a single nucleon cannot be separated from events involving 2p2h interactions or those in which first a pion was created that was subsequently reabsorbed. Thus, any theoretical description of experimental data requires a simultaneous and consistent treatment of several different elementary interaction processes.

Presently running (T2K [19], NOvA [20]) or planned (DUNE)[18] oscillation experiments aim at a precise determination of the neutrino mixing parameters, of a CP violating phase and of the mass ordering of neutrinos; they all use nuclei as targets. The oscillation formulas used to extract these quantities from the data all involve the incoming neutrino energy. This incoming energy must be reconstructed from the measured final state of the neutrino-nucleus reaction. Because of experimental acceptance cuts and the entanglement of different elementary processes this reconstruction is less than trivial. It involves an often wide extrapolation from the actually measured final state to the full final state.

An illustrative example for the typical errors in energy reconstruction is shown in Figure 1. Here a generator, in this case GiBUU [22, 23], has been used to generate millions of events as a function of 'true' energy. These events were then analyzed and the energy was reconstructed by using the so-called kinematical method. The peak of the oscillated event distribution lies at about 0.65 GeV; here the true and the reconstructed curves differ by about 25%. This discrepancy is just as large as the sensitivity of the electron appearance signal to the CP violating phase  $\delta_{CP}$ . This is illustrated for exactly the same reaction (T2K flux on  $^{16}\text{O}$ ) in Figure 1.

At the peak of the oscillation signal the curves corresponding to three different values of  $\delta_{CP}$  differ by about 25%, i.e. just by about the same amount as the error in the energy reconstruction. The influence of this error on neutrino mixing parameters has been quantified in Ref. [24, 25].

For the example shown in Fig. 1 the so-called kinematical method was used to reconstruct the energy. In this method one uses only the kinematics of the outgoing lepton, under the assumption that the reaction process was QE scattering. The higher energy experiments tend to use the calorimetric energy reconstruction since the separation of QE and pion production processes becomes the more difficult the higher the energy is. The calorimetric method relies on determining the total energy of all particles in the final state of the reaction. One immediate complication is that detectors have acceptance thresholds and that modern experiments often do not see any neutrons in their final state. Thus, the actually measured energy has to be extrapolated to the true one.

To perform this extrapolation and reconstruction so-called neutrino generators have been constructed early on. These generators try to take not only the initial neutrino-nucleon interaction into account, but also the quite essential final state interactions and

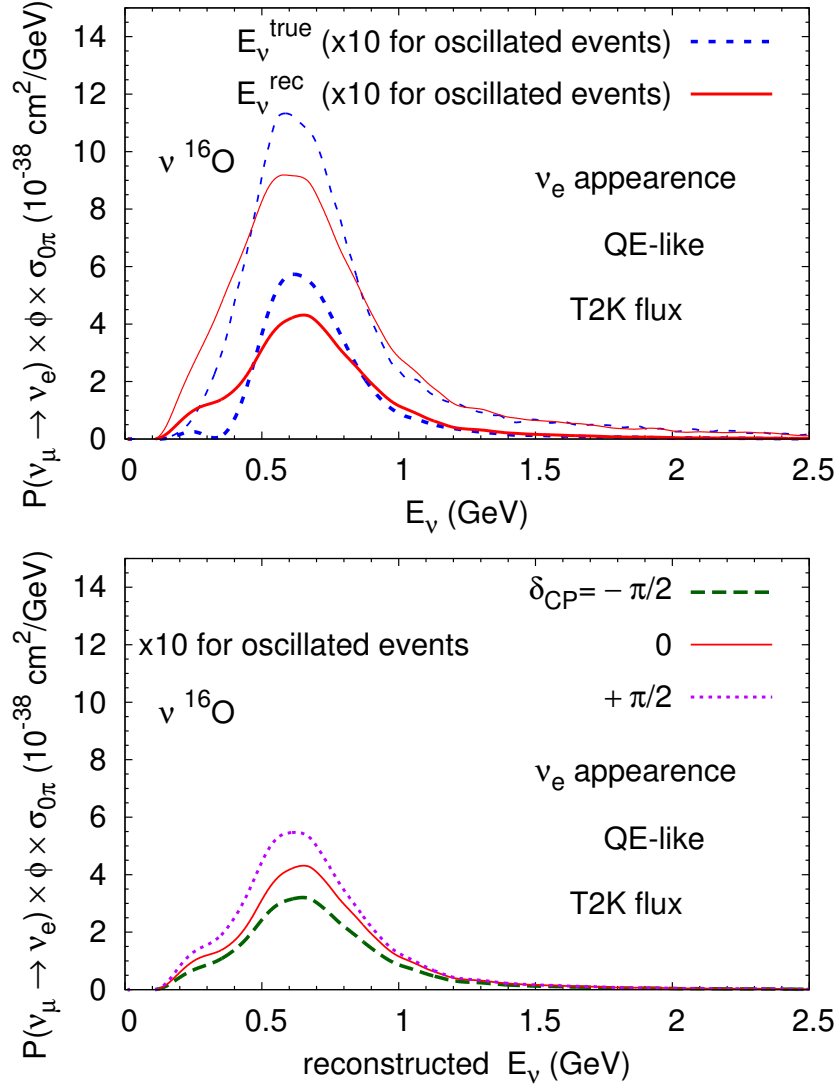


**Figure 1.** Top: QE-like event distributions for the original (thin curves) and oscillated (thick curves) in the T2K flux for electron neutrino appearance experiments, as obtained from GiBUU. The dashed curves give the event distributions as function of the true incoming neutrino energy, the solid curves those as a function of reconstructed energies. The oscillated event curves have been multiplied by a factor of 10 to enhance the visibility of the difference.

Bottom: Sensitivity of QE-like event distributions on the CP violating phase. The solid (red) curve is the same as the one in the upper part. From [21].

the geometries of the extended neutrino target. A good review of generators presently used by experiments is given in [26]. While the generator NEUT [27] is primarily being used by the T2K experiment, the generator GENIE [28, 29] has become widely used by groups connected to Fermilab experiments, such as MicroBooNE, NOvA and MINERvA. In addition, a generator named NuWro [30] is being used for comparisons of experiment with calculations. Also a transport theoretical framework, GiBUU [22, 23], for general nuclear reactions can be applied to neutrino interactions with nuclei to assess

the validity and reliability of these generators.

Obviously, in all these generators cross sections both for the initial neutrino-nucleon reaction and for the hadron-hadron reactions in the final state are essential [31]. Unfortunately, the few data that exist on elementary targets, such as p and D, are all at least 30 years old and carry large uncertainties. Our knowledge about these cross sections has been discussed in a number of fairly recent reviews [32, 33, 34].

In this article I will, therefore, not repeat the discussions of cross sections, but instead first give a short outline of the theoretical basis for any generator and discuss the approximations that go into various presently used ones. I will then go through the various subprocesses (QE, Resonance excitation, DIS, ...) and confront the inner workings of the generators with present-day nuclear physics knowledge about these processes. Towards the end of this critical review I will argue that in view of the upcoming high-precision experiments also high-precision generators are needed that are free of many the shortcomings of presently used ones.

## 2. Foundations of generators

In this chapter I briefly discuss the theoretical basis of *all* generators. Most of the generators treat the hadrons as billiard balls following classical trajectories. It is, therefore, essential to understand under which circumstances such a treatment can be justified. In the following subsection I merely summarize the essential steps necessary to get to a well-founded transport equation; more details can be found in [23, 35, 36, 37].

### 2.1. Short derivation of a general transport equation

The dynamical development of any quantum mechanical many-body system is determined by an infinite set of coupled equations for the Green's functions: the one-particle Green's function depends on the two-particle one, the two-particle Green's function depends on the higher-order one, and so on. All the higher order Green's functions can formally be included in a self-energy. The dynamics of the correlated many-body system is then determined by a Dyson equation for the single particle Green's function which contains the (quite complicated) self-energy. In addition, interaction vertices of single particles can be dressed.

Now approximations are introduced:

- The first, and most important, approximation is to truncate the hierarchy of coupled Green's functions by neglecting all higher-order correlations and keeping only the single-particle Green's function. Better is the so-called Dirac-Brueckner-Hartree-Fock (DBHF) approach in which some two-body correlations are being taken into account.
- It is, furthermore, assumed that all particles move locally in a homogeneous medium, with corresponding self-energies (potentials). This is the so-called local-density approximation.

Closely connected with the local-density approximation is the 'gradient-approximation' in which it is assumed that the Green's functions  $G(x, x')$  are rapidly oscillating functions of the relative coordinates  $x - x'$  while their variation with the center of mass coordinate  $X = (x + x')/2$  is small<sup>‡</sup>. This is the case if the medium itself is nearly homogeneous. For a nuclear system it implies that this approximation is the better the heavier the nucleus is; in heavy nuclei the homogeneous volume part prevails over the inhomogeneous surface region.

- The damping terms, i.e. the widths, of all the particles in medium are small relative to the mass gap. In nuclear physics this is well fulfilled since spectral functions of nucleons inside nuclei are fairly narrow compared to the total mass [38].

For a lepton-nucleus reaction the starting point are the single particle Green's functions for the nucleons in the target and the incoming lepton. In a homogeneous system it is advantageous to introduce the so-called Wigner-transforms of a single particle Green's function

$$\begin{aligned} G_{\alpha\beta}^<(x, p) &= \int d^4\xi e^{ip_\mu\xi^\mu} (i) \langle \bar{\psi}_\beta(x + \xi/2) \psi_\alpha(x - \xi/2) \rangle \\ G_{\alpha\beta}^>(x, p) &= \int d^4\xi e^{ip_\mu\xi^\mu} (-i) \langle \psi_\alpha(x - \xi/2) \bar{\psi}_\beta(x + \xi/2) \rangle \end{aligned} \quad (1)$$

which depend on the Dirac indices. These are the objects that determine the time-evolution in a lepton-nucleus reaction. They are nothing else than the relativistic one-body density matrices. By tracing over the Dirac indices (i.e. concentrating on the spin-averaged behavior) one obtains a vector current density

$$F_V^\mu(x, p) = -i \text{tr} (G^<(x, p) \gamma^\mu) . \quad (2)$$

The time development of the vector current density for Dirac particles, i.e. leptons and nucleons, is then given by

$$\begin{aligned} \partial_\mu F_V^\mu(x, p) - \text{tr} [\Re \Sigma^{\text{ret}}(x, p), -iG^<(x, p)]_{\text{PB}} \\ + \text{tr} [\Re G^{\text{ret}}(x, p), -i\Sigma^<(x, p)]_{\text{PB}} = C(x, p) . \end{aligned} \quad (3)$$

with

$$C(x, p) = \text{tr} [\Sigma^<(x, p) G^>(x, p) - \Sigma^>(x, p) G^<(s, p)] . \quad (4)$$

In Eq. (3) the symbol  $[\dots]_{\text{PB}}$  stands for the Poisson bracket

$$[S, G]_{\text{PB}} = \frac{\partial S}{\partial p} \frac{\partial G}{\partial x} - \frac{\partial S}{\partial x} \frac{\partial G}{\partial p} \quad (5)$$

and the quantities  $\Sigma$  in (3) are self-energies.

In a homogeneous system of fermions one can relate the two propagators  $G^>$  and  $G^<$  to each other

$$\begin{aligned} iG^<(x, p) &= +2f(x, p) \Im G^{\text{ret}}(x, p) \\ iG^>(x, p) &= -2(1 - f(x, p)) \Im G^{\text{ret}}(x, p) , \end{aligned} \quad (6)$$

<sup>‡</sup> Here  $x$  is the space-time four-vector

where  $f(x, p)$  is a Lorentz-scalar function. The trace over the imaginary part of the retarded propagator in (6) is – up to some numerical factors – just the single particle spectral function  $A(x, p)$  so that one has from (2)

$$F(x, p) = F_V^0(x, p) = 2\pi f(x, p)A(x, p). \quad (7)$$

The physics interpretation of  $F(x, p)$  is then clear from the observation that  $F_V$  is the vector density. Thus  $F$ , being the zeroth component, is the actual density distribution function in the eight-dimensional phase space  $(x, p)$ . It thus describes the time-development also of off-shell particles. Since it contains also the spectral function, often  $F$  is called the 'spectral phase space density' whereas  $f(x, p)$  is just the 'phase space density'.

The equation of motion for  $F_V$  can now be converted into one for  $F$ . It becomes

$$\mathcal{D}F(x, p) + \text{tr} [\Re G^{\text{ret}}(x, p), -i\Sigma^<(x, p)]_{\text{PB}} = C(x, p) \quad (8)$$

with

$$\mathcal{D}F = [p_0 - H, F]_{\text{PB}} \quad (9)$$

with  $H$  being the single particle Hamiltonian which involves Lorentz-scalar and -vector potential mean fields (including in particular the Coulomb field). This so-called 'drift term' (9) originates in the first Poisson bracket of Eq. (3). Using Eqs. (6) and (7) the term  $C(x, p)$  on the rhs of Eq. (8) becomes

$$C(x, p) = 2\pi g \text{tr} \left\{ [\Sigma^<(x, p)f(x, p) - \Sigma^>(x, p)(1 - f(x, p))] A(x, p) \right\}. \quad (10)$$

This term has the typical structure of a loss term (1. term in parentheses) that is proportional to the phase-space density of the interacting particle and a gain term (2. term) that takes the Pauli-principle into account. The self-energies  $\Sigma^{\gtrless}$  contain the transition probabilities for both processes.

The physics content of the second term on the left hand side of Eq. (8) is not obvious. It is also not easy to handle numerically since the term does not explicitly contain the spectral phase space density  $F$ . A major simplification was achieved by Botermans and Malfliet [39] who showed that this term can be evaluated under the assumption of local equilibrium in phase space and the gradient approximation. The equation of motion for  $F$  then becomes

$$\mathcal{D}F(x, p) - \text{tr} \left\{ \Gamma(x, p)f(x, p), \text{Re} G^{\text{ret}}(x, p) \right\}_{\text{PB}} = C(x, p). \quad (11)$$

Now the second term on the lhs is proportional to  $F$  thus simplifying its practical evaluation. The quantity  $\Gamma(x, p)$  is the imaginary part (width) of the retarded selfenergy. This shows that this term is connected to the in-medium width and is essential for offshell transport: its presence ensures that, e.g., the in-medium spectral function of a nucleon becomes a  $\delta$ -function when the nucleon leaves the nucleus.

Eq. (11) represents the center piece of a practical off-shell transport theory; it is, e.g., encoded in the generator GiBUU [22, 23]. For each particle there is one such equation to be solved and they are all coupled through the collision term, on one hand, and by the mean field potentials in  $H$  (to which all particles contribute), on the other hand. If particles, such as e.g. pions, are created in a collision the corresponding equation for them has to be added to the initial system of equations §. For an explicit example consider the case of a neutrino-nucleus interaction: initially then there is one such equation for the incoming neutrino with a  $\delta$ -function like spectral function ( $\Gamma = 0$ ) and  $A$  equations which contain the spectral phase-space densities of the nucleons in the nuclear ground state; their spectral functions are contained in  $F$  and in the Botermans-Malfliet off-shell transport term.

At this point it is worthwhile to point out that the theory developed so far as expressed in Eq. (8) is fully relativistic and the equations of motion are covariant.

*2.1.1. Initial conditions* The initial conditions for the integrations of the transport equation of motion (11) are determined by the spectral phase-space density at time  $t = 0$

$$F(x, p)_{t=0} = 2\pi f(\mathbf{x}, 0, p)A(\mathbf{x}, 0, p) . \quad (12)$$

and is thus fully determined by the Wigner-transform of the one-body density matrix. This density matrix could be obtained from any nuclear many-body theory.

## 2.2. Numerical methods

The generalized BUU equation (11) can be solved numerically by using the test-particle technique, i.e., the continuous Wigner function is replaced by an ensemble of test particles represented by  $\delta$ -functions,

$$F(x, p) = \lim_{n(t) \rightarrow \infty} \frac{(2\pi)^4}{N} \sum_{j=1}^{n(t)} \delta[\mathbf{x} - \mathbf{x}_j(t)] \delta[\mathbf{p} - \mathbf{p}_j(t)] \delta[p^0 - p_j^0(t)] , \quad (13)$$

where  $n(t)$  denotes the number of test particles at time,  $t$ , and  $\mathbf{x}_j(t)$  and  $p_j(t)$  are the coordinates and the four-momenta of test particle  $j$  at time  $t$ . As the phase-space density changes in time due to both, collisions and the Vlasov dynamics, also the number of test particles changes throughout the simulation: in the collision term, test particles are destroyed and new ones are created. At  $t = 0$  we start with  $n(0) = N \cdot A$  test particles, where  $A$  is the number of physical particles and  $N$  is the number of ensembles (test particles per physical particle). More details about the numerical treatment of the Vlasov and collision dynamics can be found in [23].

While this method is well established for the drift term of the BUU equation the collision term requires some more refinement. Here one has classically just used a geometrical argument to relate a cross section between two particles  $\sigma = \pi d^2$  to an

§ For bosons, e.g. pions, the equation actually looks slightly different, see [23]



interaction distance  $d$ . This recipe poses a problem when the energies of the interacting particles become relativistic since then the distance seen from either one of the two particles may be different in their respective restframes because there are two different eigentimes for the two particles involved whereas the equation itself contains only the laboratory time. However, in the context of heavy-ion collisions approximate schemes have been developed that minimize this problem; these same methods can also be used in neutrino generators. Other schemes involve interactions between all particles in a given phase-space cell [40]; any relativistic deficiencies can be minimized that way. The actual choice of a particular reaction channel is then done by a cross section weighted random decision.

### 2.3. Approximations

*2.3.1. Quasiparticle approximation* In the quasiparticle approximation one neglects the width of the single particle spectral function of all particles. This gives

$$F(x, p) = 2\pi g \delta[p_0 - E(x, \mathbf{p})] f(x, \mathbf{p}) \quad (14)$$

Here  $E(x, \mathbf{p})$  is the energy of a particle in mean field that depend on  $x$  and  $\mathbf{p}$  and  $g$  is the spin-isospin degeneracy. In this approximation the off-shell transport term in (11) disappears and the equation becomes for a  $2 \rightarrow 2'$  collision

$$\begin{aligned} \left[ \partial_t + (\nabla_{\mathbf{p}} E_{\mathbf{p}}) \cdot \nabla_x - (\nabla_x E_{\mathbf{p}}) \cdot \nabla_{\mathbf{p}} \right] f(x, \mathbf{p}) &= \frac{g}{2} \int \frac{d^3 \mathbf{p}_2 d^3 \mathbf{p}'_1 d^3 \mathbf{p}'_2}{(2\pi)^9} \frac{m_{\mathbf{p}}^* m_{\mathbf{p}_2}^* m_{\mathbf{p}'_1}^* m_{\mathbf{p}'_2}^*}{E_{\mathbf{p}}^* E_{\mathbf{p}_2}^* E_{\mathbf{p}'_1}^* E_{\mathbf{p}'_2}^*} \\ &\times (2\pi)^4 \delta^{(3)}(\mathbf{p} + \mathbf{p}_2 - \mathbf{p}'_1 - \mathbf{p}'_2) \delta(E_{\mathbf{p}} + E_{\mathbf{p}_2} - E_{\mathbf{p}'_1} - E_{\mathbf{p}'_2}) \\ &\times \overline{|\mathfrak{M}_{p p_2 \rightarrow p'_1 p'_2}|^2} [f(\mathbf{p}'_1) f(\mathbf{p}'_2) \bar{f}(\mathbf{p}) \bar{f}(\mathbf{p}_2) - f(\mathbf{p}) f(\mathbf{p}_2) \bar{f}(\mathbf{p}'_1) \bar{f}(\mathbf{p}'_2)] \end{aligned} \quad (15)$$

with  $E_p = E(x, \mathbf{p})$  and  $\bar{f} = 1 - f$ . The transition probability averaged over spins of initial particles and summed over spins of final particles is denoted by  $\overline{|\mathfrak{M}_{p p_2 \rightarrow p'_1 p'_2}|^2}$ . The stars "\*" denote in-medium masses and energies that involve potentials. The corresponding expressions for other collisions, such as  $2 \rightarrow 3$ , or the decay of a resonance  $1 \rightarrow 2 + 3$  can be found in [23].

The quasiparticle approximation describes a system of particles that move in a potential well. This is thus obviously a reasonable description not only of a nuclear groundstate, but also the final state interactions that take place in this same potential. The phase-space distributions  $f(x, \mathbf{p})$  are the same in the drift term as in the collision term. If many different reaction channels are open, e.g. at T2K energies CCQE scattering and  $\Delta$  resonance excitation, the collision term consists of a sum of terms for the various reaction processes. Essential is that for each individual process the initial groundstate distribution  $f$  is the same.

In the quasiparticle approximation one neglects the in-medium spectral function of particles. For nucleons this essentially amounts to neglecting their short-range correlations that are known to lead to a broadening of the nucleon's spectral function.

For in vacuum unstable particles, which have already a free width (e.g. the  $\Delta$  resonance), one has two possibilities: one can either treat these particles only as intermediate, virtual excitations that contribute to the transition matrix elements in the collision term, but are never explicitly propagated. For very broad, i.e. very short-lived, resonances this is a reasonable assumption. On the other hand, a resonance such as the  $\Delta$  lives long enough to be propagated as an actual particle. This propagation could then be handled by propagating  $\Delta$ s with different masses, but it requires some knowledge about  $\Delta N$  interactions in the collision term.

*2.3.2. Frozen approximation* The mean field potentials contained in the Hamiltonian  $H$  in (15) depend self-consistently (in a Hartree-Fock sense) on the phase-space distributions of the target nucleons. If nucleons are being knocked out by the incoming neutrino then also the mean field changes. To take care of this time-dependent change of the target structure requires some numerical expense.

A significant computational simplification can be reached by assuming that the interaction is not violent enough to disrupt the whole nucleus, but allows just for the emission of a few ( $\approx 2 - 3$ ) nucleons for nuclei with a mass number  $A > 12$ . In this case it is reasonable to assume that the nuclear density distribution does not change significantly with time ("frozen approximation", sometimes also called "perturbative particle method"). Since at the same time the number of ejected particles is relatively small collisions take place only between already ejected particles and the frozen target nucleons, but not between ejected particles. This approximation obviously becomes the better the heavier the target nucleus is and the lower the incoming neutrino energy.

The frozen approximation is used in all the generators.

*2.3.3. Free particle approximation* All neutrino generators work in the quasiparticle approximation. In addition the widely used neutrino generators do not contain any binding potentials. In these generators the nuclear ground state is not bound and the system of nucleons, initialized with a momentum distribution of either the global or the local Fermi gas model, would fly apart if the nucleons were propagated from time  $t = 0$  on. Target nucleons and ejected nucleons are thus being treated on a very different basis. While the former are essentially frozen, the latter are being propagated from collision to collision in the final state interactions. The phase-space distributions of all nucleons are always those of free nucleons with free dispersion relations connecting energy and momentum. This makes it numerically simple to follow the nucleons in the final state because in between collisions they move on straight-line trajectories. Binding energy effects are at the end introduced by fitting an overall binding energy parameter to final state energy distributions.

In this case the structure of the equation (15) is quite transparent. Assuming for

simplicity free on-shell particles one has [23]

$$\begin{aligned} H &= p^2/(2M) \\ F(x, p) &= 2\pi g \delta(p_0 - E) f(x, \mathbf{p}) \end{aligned} \quad (16)$$

where  $g$  is a spin-isospin degeneracy factor. Inserting this into (15) gives

$$\left( \partial_t + \frac{\mathbf{p}}{M} \cdot \nabla_x \right) f(x, \mathbf{p}) = C(x, \mathbf{p}) . \quad (17)$$

In this equation all potentials and spectral functions are neglected, except for the collision term it describes the free motion of particles and is used in most simple Monte-Carlo based event generators. Setting the function  $f(\mathbf{x}, \mathbf{p}) \sim \delta(\mathbf{x} - \mathbf{x}(\mathbf{t})) \delta(\mathbf{p} - \mathbf{p}(t))$  then just gives the trajectories  $(\mathbf{x}(\mathbf{t}), \mathbf{p}(t))$ , of freely moving particles (in the absence of the collision term).

While GiBUU and FLUKA [41] similarly have potentials for the nucleons implemented none of the other generators (GENIE, NEUT, NuWro) does. A prize one has to pay for the presence of potentials is in terms of computer time: in between collisions the nucleons move on trajectories that are determined by the potentials; these trajectories have to be numerically integrated, if potentials (including Coulomb) are present.

#### 2.4. Factorization in $\nu A$ reactions

In a neutrino-nucleus reaction the incoming neutrino first reacts with one (or two) nucleons which are bound inside the target nucleus and are Fermi-moving. The reaction products of this very first reaction then traverse the nuclear volume until they leave the nucleus on their way to the detector. This time-development suggests to invoke the so-called factorization of the whole reaction into a first, initial process and a final state interaction process. The factorization is, however, not perfect. The wave functions of the outgoing nucleons from the first, initial interaction, and thus the cross sections for this initial interaction, are influenced by the potentials present in that final state. The subsequent propagation of particles then takes place in this very same potential.

This is not the case in the generators which decouple the first interaction from the final state ones. For example, in some versions of GENIE, NEUT and NuWro the spectral functions of nucleons are taken into account in the description of the initial state for the very first interaction. These spectral functions contain implicitly information on potentials and off-shellness. However, the outgoing nucleons move freely on straight lines, i.e. without experiencing a potential, and only their energies are corrected by some constant binding energy. This is obviously not consistent. A consistent theory requires to use the full off-shell transport for these 'collision-broadened' nucleons if one is interested not only in semi-inclusive cross sections, but also in quantities such as the final momentum-distribution of the hit nucleon.

### 2.5. Preparation of the target ground state

The nuclear ground state plays an important role for neutrino-nucleus interactions. In most generators it is simply assumed to be described by a free Fermi gas, either global or local. This ansatz neglects all effects of nuclear binding; the nucleus, if left alone, would simply 'evaporate'.

From studies of p-A scattering one knows that the nucleon-nucleus potentials are momentum-dependent such that at small momenta ( $< p_F$ ) they produce binding and at larger kinetic energies of about 300 MeV they disappear [42].

In the nuclear many body approach [2] all the effects of a binding potential are contained in the spectral function, even though the potentials themselves cannot be easily determined. The scaling models, on the other hand, do not really need a groundstate if the scaling function has been determined from experiment. On the other hand, in the SUSA approach it is explicitly calculated from a relativistic mean field theory [43]; its properties then are used in calculating the scaling function. In these calculations the potential is momentum-dependent.

In GiBUU the ground state is prepared by first calculating for a given realistic density distribution a mean field potential from a density- and momentum-dependent energy-density functional, originally proposed for the description of heavy-ion reactions [44]. The potential obtained from it is given by

$$U[\rho, p] = A \frac{\rho}{\rho_0} + B \left( \frac{\rho}{\rho_0} \right)^\tau + 2 \frac{C}{\rho_0} \int d^3 p' \frac{f(\vec{r}, \vec{p}')}{1 + \left( \frac{\vec{p} - \vec{p}'}{\Lambda} \right)^2} \quad (18)$$

which is explicitly momentum dependent. Here  $\rho_0$  is the nuclear equilibrium density and  $f(\vec{r}, \vec{p}')$  is the nuclear phase-space density. If a local Fermi-gas model is used it reads

$$f(\vec{r}, \vec{p}') = \frac{4}{(2\pi)^3} \Theta[|\vec{p}'| - p_F(\vec{r})] \quad \text{with} \quad p_F = \left( \frac{3}{2} \pi^2 \rho(\vec{r}) \right)^{1/3}; \quad (19)$$

it is consistent with the spectral phase-space density defined in Eq. (12) for a local Fermi gas momentum distribution, neglecting any in-medium width of the nucleons. By an iterative procedure the Fermi-energy is constant kept constant over the nuclear volume; the binding is fixed to -8 MeV for all nuclei.

The parameters appearing in this potential are given for two different parameter sets in a Table in Ref. [45]. Typical potentials are shown in Figure 2 in their dependence on momentum  $p$ .

The potentials EQS5 and EQS14 agree with each other in the kinetic energy range  $100 < T < 300$  MeV. For lower kinetic energies, corresponding to lower energy transfers, EQS5 gives a better description of the data (see the results shown in [46]).

In addition to the nuclear potential just discussed for charged particles there is also a Coulomb potential present, which is also implemented in GiBUU, but in none of the other generators. Both potentials together affect mainly low momentum particles. They

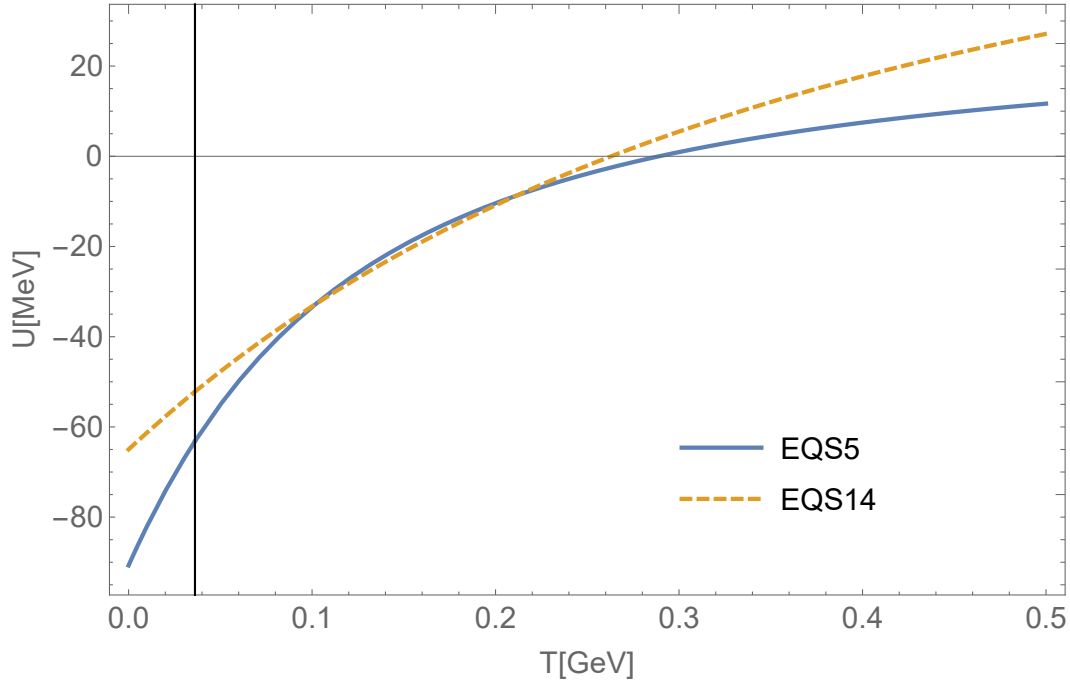


**Figure 2.** The two potentials corresponding to the parametersets EQS5 (solid) and EQS14 (dashed) at density  $\rho_0 = 0.16 fm^{-3}$  as a function of kinetic energy. The solid vertical line indicates the kinetic energy at the Fermi surface. EQS14 (dashed) is obtained from a fit to experimental pA data [42] at  $r = 0$ .

also cause a deviation of final state particle's trajectories from straight lines which are usually assumed in standard generators.

*2.5.1. RPA correlations* In calculations that start from an unbound initial state with a local Fermi gas momentum distribution it was found that RPA correlations play a major role in the region of the QE peak. Here, at reasonably small  $Q^2 \approx 0.2 \text{ GeV}^2$  uncorrelated calculations were found to describe the data already reasonably well. Adding then RPA effects was found to lower the cross section by about 25%; after adding then the 2p2h contributions, to be discussed in a later subsection, agreement with the data was again achieved [47].

Only recently the Ghent group has shown that this strong lowering caused by the RPA correlations is mostly an artifact due to the use of an unphysical ground state in these calculations [48]; this was most recently also confirmed in an independent calculation [49]. In Continuum RPA (CRPA) calculations this group showed that RPA effects overall are significantly smaller and play a significant role only at small  $Q^2$  and very small energy transfers when a realistic groundstate potential is used. This result provides a justification for using mean field potentials in generators without any RPA correlations. Fig. 3) shows a comparison of the double-differential cross section for the QE scattering of the MicroBooNE flux on  $^{40}\text{Ar}$ . The overall agreement between models is quite good and illustrates the small influence of RPA correlations on dd semi-inclusive

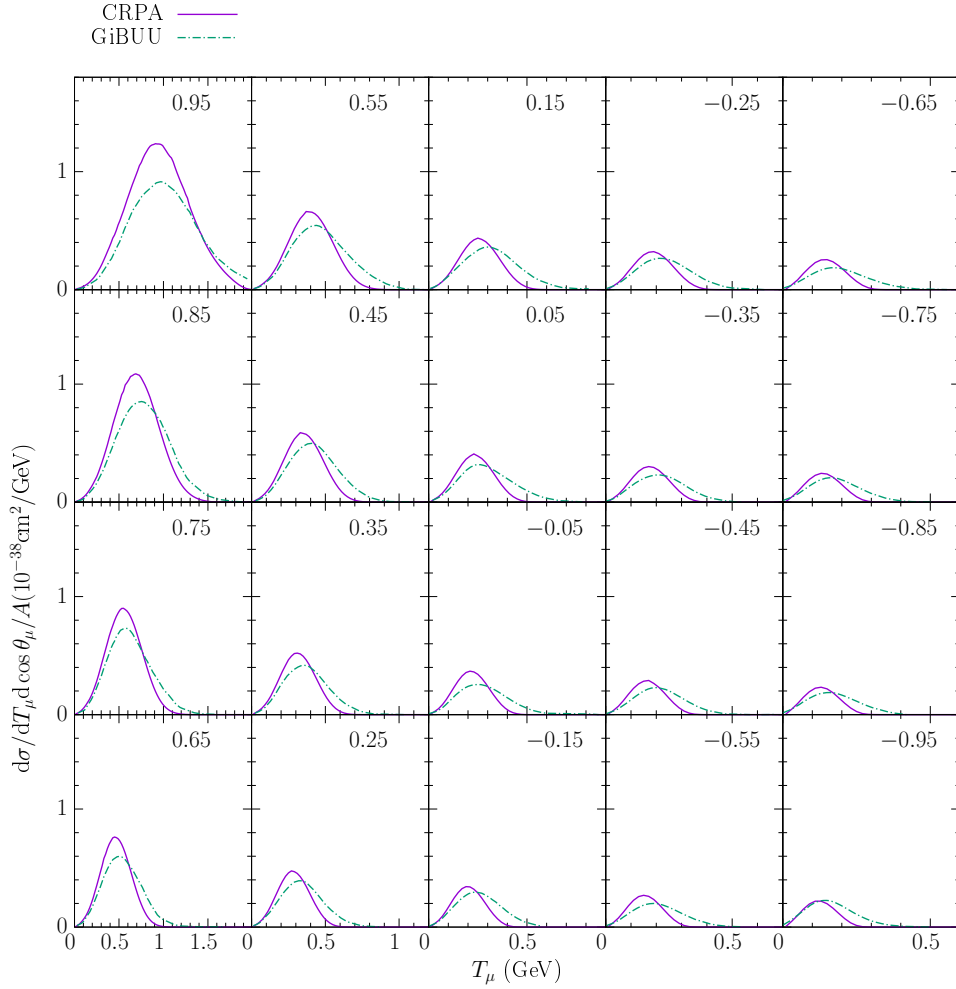


**Figure 3.** Double-differential QE cross section for outgoing muons in a reaction of neutrinos in the booster neutrino beam with  $^{40}\text{Ar}$ . The numbers in the upper parts of each subfigure gives the cosine of the muon scattering angle with respect to the neutrino beam. All cross sections are given per nucleon. The solid curve gives the results of a CRPA calculation [50], the dash-dotted curve those obtained with GiBUU.

cross sections. Since in the calculations of Ref. [47] the strong RPA effect was nearly canceled by an equally strong, but with opposite sign, effect of 2p2h interactions one could speculate that also the latter were over-estimated in a calculations that starts with a free, non-interacting ground state.

*2.5.2. Spectral functions* Nuclear many-body theory obtains the hole spectral function  $\mathcal{P}_h(\mathbf{p}, E)$  which contains all the information about the energy-momentum relation of a bound particle [2]. This is just given by the distribution function  $F(x, p)_{t=0}$  in Equation (12), i.e. by the one-body density matrix. In the quasiparticle approximation this becomes

$$F(\mathbf{x}, t = 0, p) = 2\pi g \delta[p_0 - E(\mathbf{x}, \mathbf{p})] f(\mathbf{x}, t = 0, \mathbf{p}) . \quad (20)$$

This quasiparticle approximation – used together with the global Fermi gas momentum distribution – has been criticized because it leads to ‘spiky’,  $\delta$ -function shaped energy-momentum distributions. This, however, is a problem only for free particles without any potential. In that case we have  $E(\mathbf{x}, \mathbf{p}) = \sqrt{\mathbf{p}^2 + m^2}$ . Then the energy  $E$ , and therefore also  $F$ , is no longer dependent on  $\mathbf{x}$  so that the spiky behavior is also present after integration over the nuclear volume. If there is a potential present, however, then the hole spectral function is much better behaved even if the momentum distribution is given by a Fermi-gas approximation. We illustrate this here for a local Fermi gas bound in a scalar potential. In this case the groundstate distribution function  $f(\mathbf{x}, t = 0, \mathbf{p})$  is given by

$$f(\mathbf{x}, \mathbf{p})_{t=0} = \frac{1}{(2\pi)^3} \int d^3s e^{-i\mathbf{p}\cdot\mathbf{x}} \rho(\mathbf{x} - \frac{\mathbf{s}}{2}, \mathbf{x} + \frac{\mathbf{s}}{2}), \quad (21)$$

i.e. just by the Wigner transform of the single particle density matrix. The hole spectral function  $\mathcal{P}_h(\mathbf{p}, E)$  can be obtained, e.g., from nuclear many-body theory (NMBT) [2, 2]. As a simpler alternative, in semi-classical theory it is given by

$$\mathcal{P}_h(\mathbf{p}, E) = g \int_{\text{nucleus}} d^3x \Theta[p_F(\mathbf{x}) - |\mathbf{p}|] \Theta(E) \delta\left(E - m^*(\mathbf{x}, \mathbf{p}) + \sqrt{\mathbf{p}^2 + m^{*2}(\mathbf{x}, \mathbf{p})}\right), \quad (22)$$

here  $g$  is a degeneracy factor and  $p_F$  is the local Fermi-momentum taken to be a function of  $p_F(\mathbf{x}) \sim \rho(\mathbf{x})^{1/3}$  (local Fermi-gas). For simplicity it is assumed that in this spectral function all effects of the nucleon potential are contained in the effective mass  $m^*$  [23] which can depend on location and momentum of the nucleon. The corresponding *momentum distribution* approximates that obtained in state-of-the-art nuclear many-body theory calculations quite well (see Figure 4 in [51]); its *energy distribution* no longer contains the  $\delta$ -function spikes of a free Fermi gas because of the  $\mathbf{x}$ -dependence of the potential in  $m^*$  and the integration over  $d^3x$ .

## 2.6. Calorimetric energy reconstruction

There are two methods known to reconstruct the energy of the incoming neutrino from final state properties:

- **Kinematical method.** In this method one uses the fact that the incoming energy of a neutrino interacting in a CCQE process with a neutron at rest is entirely determined by the kinematics of the outgoing lepton. If this method is used with nuclear targets then there are two complications: first, the neutron is not free and at rest, but it is bound in a nucleus and Fermi moving. This alone already leads to a smearing of the reconstructed energy around the true one. Also, the method in principle requires to identify the interaction process as true QE scattering. This, however, is impossible in a nuclear target where always pion production followed by reabsorption takes place if the incoming energy is high energy. This effect leads to a low-energy tail in the reconstructed energy [52]. The same is true for any

other interaction process [21]. Therefore, the method is expected to work best at lower energies, such as in the T2K or the BNB beams, where only QE, 2p2h and  $\Delta$  excitation contribute. These three processes then have to be described well by the generator.

- **Calorimetric method.** In this method one measures the energies of all particles in the final state and reconstructs the energy from that information. Problems with this method arise because detectors are not perfect, have detection threshold and may miss certain particles, e.g. neutrals, altogether. The energy then has to be reconstructed from a final state that is only partially known.

An often not discussed problem in this method is connected with the final state of the target remnant. The nucleons in the target nucleus carry energy and momentum which have to enter into the overall energy-conservation, both in the initial and the final state. Similarly, in a final state collision between the primarily ejected nucleon and a target nucleon the energy and momentum of the latter also enter into the energy-momentum conservation condition, but in the usually used frozen configuration they are not taken into account.

### 3. Reaction types

#### 3.1. Coherent interactions

An incoming neutrino can interact with the nucleus in many different ways. It can, first of all, coherently interact with all nucleons. This process happens if the momentum transfer is small and can lead either to elastic neutrino scattering (in a Neutral Current (NC) event) [53] or to coherent pion production where the pion carries off the charge of the  $W$  in a CC event [54]. In both reaction types the target nucleus remains in its groundstate. Such processes can be described by a coherent sum over the individual nucleon amplitudes [55] and thus depends crucially on a phase-coherence between all nucleons. This coherence cannot be described by the Green's function formalism discussed above which describes the incoherent time-evolution of single particle phase-space densities. Thus, coherent processes fall outside the validity of any semi-classical description and have to be added 'by hand' to any generator.

Theories for the description of coherent processes have been developed for incoming on-shell photons [56] and experimental results for these are available [57]. For neutrino-induced coherent processes the situation is more complicated since experiments usually cannot see deexcitation photons from the target nucleus; one can thus not be sure that the target is left in its ground state. Theoretical investigations of coherent neutrino-induced pion production exploit the fact that the incoming gauge boson 'sees' a coherent superposition of all nucleons and, therefore work with the overall form factor of the target nucleus [58, 54]. This is clearly an advantage in particular at higher energies where fully microscopical calculations such as the one in [55] are not feasible because of the large number of contributing states.



### 3.2. Semi-inclusive cross sections

The transport equations describe the full event evolution, from the very first, initial interaction of the incoming neutrino with one (or more) nucleons through the final state interactions up to the asymptotically free final state consisting of a target remnant and outgoing particles.

Semi-inclusive cross sections as a function of the outgoing leptons's energy and angle (or equivalently  $Q^2$  and  $\omega$ ) are then easily obtained by stopping the time-evolution after the first initial interaction. They are defined as the sum of cross sections for all microscopic initial processes. Knowledge about the final fate of the initially struck particles is not required for determining that quantity. Such semi-inclusive cross sections obviously are a necessary test for all theoretical descriptions of neutrino-nucleus interactions. In the theoretical framework outlined above they are obtained by summing over all reaction processes in the first time-step; the further time-development of the reaction is irrelevant for these inclusive cross sections. For example, for the semi-inclusive QE scattering cross section one has

$$d\sigma_{\text{QE}}^{\nu A}(E, Q^2, \omega) = \int \frac{d^3p}{(2\pi)^3} dE P_h(\mathbf{p}, E) f_{\text{corr}} d\sigma_{\text{QE}}^{\text{med}}(E, Q^2, \omega) P_{\text{PB}}(\mathbf{x}, \mathbf{p}) . \quad (23)$$

Here  $d\sigma^{\text{med}}$  is a possibly medium-dressed semi-inclusive cross section on a nucleon,  $f_{\text{corr}}$  is a flux correction factor  $f_{\text{corr}} = (k \cdot p)/(k^0 p^0)$ ;  $k$  and  $p$  denote the four-momenta of the neutrino and nucleon momentum, respectively and  $P_{\text{PB}}(\mathbf{x}, \mathbf{p})$  describes the Pauli-blocking. The cross section  $d\sigma$  on the lhs of Equation (23) depends on  $Q^2$  and  $\omega$  and can thus be used to calculate the semi-inclusive cross section.

Final state interactions enter into the inclusive cross sections only through the final states needed to calculate the transition amplitude in the first, initial interaction. The interactions that produced particles experience when they traverse the nucleus are irrelevant for it.

From these discussions it is clear that all generators, i.e. all theories and codes that lead to a full final state event, are also able to describe inclusive and lepton semi-inclusive cross sections. The opposite, however, is not true. Theories that describe the inclusive or semi-inclusive (as function of the outgoing lepton's energy and angle) cross sections very well but inherently integrate over all final momenta of the first interaction do not give any information about the subsequent dynamical evolution of the system. Into this category fall the so-called scaling method and the nuclear-many body theories. Both will be discussed in the following sections.

*3.2.1. Scaling models* It was observed quite early on that electron scattering data on nuclei show 'scaling' over a kinematical range that roughly covers the low  $\omega$  side of the QE-peak up to its maximum [59]. 'Scaling' here means that the ratios of the nuclear data over the nucleon data in the QE region are described by a function  $F(y)$  of the single variable  $y(q, \omega)$  which depends on the momentum transfer  $q$  and the energy transfer  $\omega$ .

Later on, the scaling function was extended to include more detailed information on the particular target nucleus by introducing the Fermi momentum  $p_F$  and a shift parameter to fit the strength and the position of the QE peak [60]. With these fit parameters an excellent description of electron data in the QE-peak region could be obtained [61]. While all these analyses relied on data models were also developed to calculate the scaling function starting from nuclear theory. This led to the quite successful SUSAv2 model [43, 62] which combines a relativistic mean field description of the target nucleus with a calculation using the Relativistic Plane Wave Impulse approximation at higher energies.

In summary, the SUSA model is an excellent tool to calculate lepton-induced inclusive and semi-inclusive cross sections on nuclei; semi-inclusive here refers to the outgoing lepton. Its main strength lies in the description of semi-inclusive cross sections in the QE region. Inelastic excitations have to be added in by using phenomenological fits to single-nucleon inelastic structure functions. The method does not give any information on the final state of the reaction, except for the outgoing lepton's properties, and thus cannot be used in any generator without invoking further approximations.

*3.2.2. Methods from nuclear many body theory* Short range correlations in nuclei cause a broadening of the nucleon spectral function which in vacuum is just given by  $\delta$  function. Nuclear many body theory (NMBT) has allowed to calculate that function for the nuclear hole states in the nuclear ground state to a high precision [5]. By invoking the impulse approximation one then uses this hole spectral function to describe the initial state in a QE scattering event; the final state in this method is usually assumed to be that of a free nucleon (impulse approximation) [2]. The calculations thus contain effects in the nuclear ground state that go beyond the mean-field approximation, e.g. short-range correlations. The semi-inclusive cross sections are then just given by Eq. (23) with the hole spectral function obtained from NMBT. The inclusive cross section is obtained by summing the total cross sections for all individual processes. Thus the reliability of this method also relies on the ability of the theory to describe besides QE scattering also pion production (for the T2K energy regime) and also higher-lying excitations and DIS processes for the DUNE flux. In presently available calculations these inelastic excitations are usually taken from fits to inclusive inelastic responses. Invoking the impulse approximation this method allows to calculate not only the semi-inclusive cross section (with respect to the outgoing lepton), but it also can give the outgoing nucleon from the first interaction, without any further final state interactions, however.

So far, furthermore, most of the results are available only for electron-induced reactions; results for neutrino-induced reactions are mostly missing. Nevertheless, the generators GENIE, NEUT and NuWro have implemented a so-called spectral function option into their description of QE scattering. In this option the very first, initial interaction is described by a cross section for QE scattering obtained by using a spectral function. Such a procedure is dubious since it uses a very different ground state for the QE scattering than for the other processes. Furthermore, in these generators the

potential for the outgoing particles is absent and there is, therefore, a discontinuity between the initial state potential, hidden in the spectral function, and the final state potential. The method can thus work only in a limited kinematic range where the outgoing nucleon's kinetic energy is about 250 - 300 MeV so that the momentum-dependent potential nearly vanishes (see Figure 2.5).

More recently, nuclear many-body theories have had a remarkable success in describing the nuclear groundstate and low-lying excitations starting from *a priori* interactions [63, 64]. Their main strength lies in calculating semi-inclusive cross sections at relatively low energies since they become the better the closer they stay to the nuclear ground state. There these calculations have the potential to describe not only the inclusive contributions of true one-particle QE events but also admixtures of 2p2h events that could overlap with the former. On the other hand, processes connected with higher-lying excitations, e.g. pion production, are, however, usually taken from fits to inclusive inelastic response data. The method, so far, does not yield any spectral functions and can thus not be combined with the impulse approximation as in the NMBT calculations. It has, however, recently also reproduced experimental results for the semi-inclusive QE response in NC events on light nuclei [64].

*3.2.3. Comparison with experiment* A quite general difficulty even for describing semi-inclusive cross sections with these methods is that experimental neutrino data always contain a superposition of many different reaction channels. In electron-induced reactions the measurable energy transfer can be used to distinguish at least the bulk parts of QE scattering and resonance excitations, for example. In neutrino-induced reactions, however, the beam energy and thus also the energy transfer is smeared (see discussion in the introduction). Thus, any events in the QE region are always mixed with those where other processes prevailed. At the lower beam energy of the T2K experiment, for example, QE and pion production through the  $\Delta$  resonance, overlap. This implies that the QE cross section alone cannot be measured in neutrino-induced reactions. This is also true for so-called 0-pion (sometimes also called QE-like) events without any pions in the final state. In this case pions could have been first produced through  $\Delta$  excitation and then reabsorbed through fsi. Detailed analyses show that the latter events amount to about 10% in the T2K energy range ( $\approx 700$ ) MeV [65]. Theories, that work well for electrons in describing the semi-inclusive cross sections around the QE peak, thus have difficulties in describing experimental neutrino-induced cross sections already at slightly higher energies, even if these are for semi-inclusive or 0 pion events.

### *3.3. Quasielastic interactions*

The simplest process that can take place in a neutrino-nucleus reaction is that of quasielastic (QE) scattering in which the incoming neutrino interacts with just one nucleon. In theoretical descriptions one usually assumes that the cross section for

that process on a Fermi-moving nucleon is the same as that on a free nucleon, except for a necessary Lorentz transformation to the moving nucleon's rest frame ("impulse approximation"). Assuming a Fermi gas momentum distribution for the initial nucleons and free movement for the final state particles allows to give an analytical expression for this cross section [12, 11]

In the early work by Smith and Moniz [11] there was the assumption hidden in that cross section that the binding energy of the hit nucleon before and after the collision can be neglected; only possible Pauli-blocking of the final state is taken into account. Binding energy effects are then simulated by a change of the energy of the final state nucleon which is assumed to be free [66]; sometimes also the energy transfer is modified [2] mainly to correct for the target recoil. Using the so-called impulse approximation then not just inclusive cross sections but also properties of the outgoing nucleons can be calculated.

This impulse approximation makes it possible to use also the spectral functions obtained from nuclear many-body theory for a description of the initial state while the final state is still assumed to be free. In terms of the general structure of the transport equations in Section 2 this procedure corresponds to a mixture of the full theory as outlined there and the quasiparticle approximation without potentials. The very first interaction is described by the interaction of the incoming neutrino with correlated and bound target nucleons described by broadened spectral functions. The following transport of the initial final state through the nuclear environment then proceeds as if the nucleons were unbound and  $\delta$ -function like in their energy-momentum dispersion relation.

In these calculations an initial state potential is inherent in the spectral function even though its precise value is not known. Assuming then a free outgoing nucleon introduces implicitly a momentum-dependence in the potential. From an analysis of  $pA$  reactions [42] it is known that the nucleon-nucleus potential is momentum dependent such that it is attractive ( $\cong -50$  MeV) at low ( $< p_F$  momenta) whereas it becomes very small at larger momenta ( $\cong -500$  MeV) (see Figure 18). Such a momentum-dependence of the single-particle potential has been known to affect the position of the QE peak [67, 68]. In [69] the authors have demonstrated that such a potential has a major influence on the location of the QE peak, in particular at low momentum transfers where the momentum dependence of the potential is strongest. Indeed, at the lowest  $Q^2$  the effect of the final state potential, which is introduced from the outside, is larger than that of the spectral function.

### 3.4. $2p2h$ processes

From earlier studies with electrons it was well known that incoming electrons can also interact with two nucleons at the same time in so-called  $2p2h$  processes [4, 70]. These interactions are often connected with an excitation of the  $\Delta$  resonance by the incoming virtual photon. They tend to fill in the so-called 'dip region' between the QE-peak and

the  $\Delta$  peak in semi-inclusive cross sections as a function of energy transfer. Shortly afterwards it was recognized by M. Ericsson et al [71, 72] that such processes can also play a role in neutrino-induced reactions, in particular if only the outgoing lepton was observed.

This knowledge was rediscovered after the data of the experiment MiniBooNE showed a surplus of so-called quasielastic-like events as a function of reconstructed neutrino energy [73]. The surplus could be explained quite well just by these 2p2h processes [47, 74, 75, 76, 77]. The models used in this work involved various assumptions, such as non-relativistic treatment, unbound local Fermi gas for the groundstate and a restriction of the underlying elementary processes to the  $\Delta$  resonance region. The latter limits the application of such models to neutrino energies less than about 1 GeV.

In the following subsections in generators two presently used models for the 2p2h contribution are discussed. A common shortcoming of both of these methods is that they give only semi-inclusive cross sections for the 2p-2h channel. For use in a generator thus an additional assumption has to be made about the momentum-distributions (energy and angle) of the final state particles. Usually a uniform phase-space occupation is imposed which can be formulated very easily in the two-particle cm system, followed by a boost to the laboratory system [78].

#### 3.4.1. Microscopic 2p2h contribution

*Microscopic model* The calculations first used to explain the MiniBooNE data used various approximations. The calculations reported in [74, 75, 76] were non-relativistic and involved further approximations such as the neglect of longitudinal contributions to the vector-axial vector interference term. The calculations reported in [47], on the other hand, were relativistic and involved approximations in evaluating the momentum-space integrals and in neglecting the direct-exchange interference terms in the matrix elements. Both models start from an unbound groundstate assuming a local Fermi-gas momentum distribution. Intrinsic excitations of the nucleon are limited to the  $\Delta$  resonance; this limits the applicability of these models to the MicroBooNE, T2K energy regime.

The model does not give information about the isospin composition of the final state nor does it provide the energy-momentum distributions of outgoing nucleons. For use in a generator it thus has to be supplemented with assumptions about these distributions.

The calculations of the Valencia group [47] have found their way into the generators GENIE and NEUT as options. It is unclear, however, to the outsider how this implementation into the existing generators was performed: were just the cross sections used or were the structure functions implemented? Unfortunately, no documentation is available. This is particularly annoying since the model of [47] is found to severely underestimate the 2p2h strength in the dip region [79] which led the MINERvA collaboration to increase its strength by multiplying it with a 2d correction function amounting to an overall factor of 1.53. A comparison of the original Valencia result or

the tuned version in GENIE with electron data and with neutrino data from another experiment would be desirable, but does not exist.

*MEC model* The most complete calculations of the 2p2h contributions that are free of the approximations just mentioned were performed in Ref. [80, 81]. These authors evaluated all the relevant diagrams involving 2p2h interactions in the nucleon and  $\Delta$  energy regime; in doing so they invoke a prescription to handle the  $\Delta$  propagator that appears in the two-body currents; only the real part of this propagator is used. The calculations are based on a free Fermi gas model for the nuclear ground state, which is thus unbound. They are fully relativistic and include all the interference terms. While earlier calculations had assumed that the 2p2h contribution was purely transverse, the new calculations by Megias et al also obtain a longitudinal contribution although the latter is small relative to the transverse one [81, 62]; it is not clear how much of it is due to the neglect of a binding potential in the initial state. These authors have combined the microscopic 2p2h cross section thus calculated with the SUSA description of QE scattering and obtain impressive agreement with semi-inclusive electron and neutrino data [82, 83] in the QE and dip region.

An additional advantage of this method is that it predicts the relative ratios of pn pairs vs pp pairs in the outgoing state [84]. This is particularly interesting because electron-induced experiments show a clear enhancement of pn vs. pp pair ejection [85]. This effect is usually ascribed to the dominance of pn pairs vs pp pairs in nuclear matter. The calculations of RuizSimo et al [86] show that at least a part of the observed effect is due to the actual interaction process.

The MEC model evaluates the two-body current with nucleons up to the  $\Delta$  resonance. This is sufficient for the T2K and MicroBooNE energy regime. It does not give any information on the momentum distribution of the outgoing particles and thus cannot be used in a generator without further additional assumptions on the final state of the 2p2h process.

*3.4.2. Empirical 2p2h contribution* An alternative to the microscopic calculations for 2p2h contributions is to take these directly from an analysis of semi-inclusive electron scattering data. An analysis by Bosted et al and Christy [87, 88] indeed did extract the structure function for these processes directly from data in a wide kinematical range ( $0 < Q^2 < 10 \text{ GeV}^2$ ,  $0.9 < W < 3 \text{ GeV}$ ) that goes well beyond the resonance region and implicitly includes any src and DIS components. Starting assumption for this extraction was that these 2p2h effects are purely transverse. The parameterized structure functions  $W_1^e(Q^2, \omega)$  thus obtained can then directly be used in calculations of cross sections for electrons. It contains not only effects of meson exchange currents, but also those of any short range correlations. In GiBUU these structure functions have been combined with the other reaction processes and good agreement with semi-inclusive electron data is obtained [46]. It is worthwhile to point out that this structure function was obtained from a fit to data in a kinematical range that goes well beyond the resonance region

and also includes DIS components.

Under the assumption that also for neutrinos the dominant 2p2h cross-section contribution ( $\sigma^{2p2h}$ ) is transverse and that lepton masses can be neglected the corresponding cross section can be written in terms of the three neutrino structure functions  $W_1^\nu$  and  $W_3^\nu$

$$\begin{aligned} \frac{d^2\sigma^{2p2h}}{d\Omega dE'} = \frac{G^2}{2\pi^2} E'^2 \cos^2 \frac{\theta}{2} & \left[ 2W_1^\nu \left( \frac{Q^2}{2\mathbf{q}^2} + \tan^2 \frac{\theta}{2} \right) \right. \\ & \left. \mp W_3^\nu \frac{E + E'}{M} \tan^2 \frac{\theta}{2} \right]. \end{aligned} \quad (24)$$

Here  $G$  is the weak coupling constant;  $E'$  and  $\theta$  are the outgoing lepton energy and angle respectively;  $E$  is the incoming neutrino energy; and  $M$  is the nucleon mass.

Walecka et al. [89, 90] have derived a connection between the electron and the neutrino structure functions. In the version used by the Lyon group [91] it reads

$$W_1^\nu = \left( 1 + \frac{G_A^2(Q^2)}{G_M^2(Q^2)} \frac{\mathbf{q}^2}{\omega^2} \right) W_1^e 2(\mathcal{T} + 1) \quad (25)$$

Here  $G_M(Q^2)$  is the magnetic coupling form factor,  $G_A(Q^2)$  the axial coupling form factor and  $Q^2$  is the squared four momentum transfer  $Q^2 = \mathbf{q}^2 - \omega^2$ . The structure of  $W_1^\nu$  is transparent: to the vector-vector interaction in  $W_1^e$  an axial-axial interaction  $G_A(Q^2)$  term is added; the axial coupling is related to the vector coupling by an empirical factor  $\mathbf{q}^2/\omega^2$  [91]. The extra factor 2 is due to the fact that neutrinos are left-handed only. Finally, a factor  $(\mathcal{T} + 1)$  appears where  $\mathcal{T}$  is the isospin of the target nucleus.

A similar structure shows up in the V-A interference structure function

$$W_3^\nu = 2 \frac{G_A}{G_M} \frac{\mathbf{q}^2}{\omega^2} W_1^e 2(\mathcal{T} + 1). \quad (26)$$

Exactly this form has also been used in all calculations by the Lyon group [74].

The isospin factor in (25) and (26) is derived under the assumption that neutrinos populate the isobaric analogue states of those reached in electron scattering. The Wigner-Eckart theorem then allows to connect the transition matrix elements for electrons ( $\sim \tau_3$ ) with those for neutrinos ( $\sim \tau_\pm$ ). This connection was originally derived by Walecka [89] for single particle processes but it also holds for the 2p2h processes considered here because the relevant transition operators can again be expressed in terms of irreducible tensors of SU(2). As already mentioned this connection depends on the assumption that neutrino processes excite just the isobaric analogues of states reached in electron scattering. It would thus be very interesting to verify the presence of this isospin factor in actual data. So far most of neutrino data were obtained for the  $\mathcal{T} = 0$  nuclei C and O. It will, therefore, be very interesting to see the effects of this factor for the isospin asymmetric nucleus  $^{40}\text{Ar}$  for which  $\mathcal{T} = 2$ . To experimentally verify this will require a very good knowledge of the incoming neutrino flux and small other uncertainties (see discussion in [46, 92]).

Equations (25) and (26) relate both the neutrino structure function  $W_1^\nu$  and the interference structure function  $W_3^\nu$  to just one other function, the structure function

$W_1^e(Q^2, \omega)$ , determined from electron data. Parameterizing the latter, either by the Bosted et al fit or by some other ansatz, as a function of  $Q^2$  and  $\omega$  then determines the electron, neutrino and the antineutrino cross sections consistently [46].

This phenomenological model does not make predictions about the magnitude of pp pair vs pn pair ejection since the phenomenological analysis, on which the model is based, did not take any final state information into account. Instead, in GiBUU which uses this phenomenological description, the isospin composition of pairs is entirely determined by statistical ratios.

Because of the wide kinematical range of the data that were used to extract  $W_1^e$  the model is applicable to experiments with high incoming energy (MINERvA, NOvA, DUNE). Since it is based on an empirical analysis of semi-inclusive 2p2h processes the model does not give any information on the final state. In GiBUU it is, therefore, supplemented with the assumption that the energy- and momentum-distributions of the two outgoing nucleons are determined by phase-space.

### 3.5. Pion production

In neutrino-nucleus reactions pion-production plays a major role. In particular at the higher energies of the MINERvA or DUNE experiment pion-production, through resonances or DIS, makes up for about 1/2 - 2/3 of the total interaction cross section. Therefore it must be under quantitative control in the generators used to extract cross sections and neutrino mixing properties from such experiments. Very recently, two comparisons of the generators NEUT (with charged pion - nucleus data) [93] and GENIE (with MINERvA neutrino-induced pion production data) [94] have shown that major discrepancies of these generators with the data exist that cannot be tuned away.

Theoretically, the pion production cross section in the resonance region is obtained as a coherent sum over resonance and background amplitudes. This in itself poses a problem for generators since these quasiclassical method cannot handle any quantum mechanical interferences between resonance and background contributions.

*3.5.1. Resonance amplitudes* The resonance amplitudes are determined by the nucleon-resonance transition currents. For the case of a spin-isospin 3/2-3/2 resonance as for the  $\Delta$ , there are three vector form factors and three axial ones. In standard neutrino generators GENIE and NEUT the so-called Rein-Segal model [95] for the form factors for resonance excitation is still used although that model is known to fail in its description of electron scattering data [96, 97]. The generator NuWRo uses a model with a formation-time parameter even in the  $\Delta$  resonance region[98]. This gives additional tuning degrees of freedom which, however, have no physical basis: In the resonance region the time-development of pion production is governed by the resonance width; there is no room for additional parameters.

A better way is to determine the vector form factors  $C_i^V(Q^2)$ , which are directly related to the electromagnetic transition form factors [99], from the measured helicity



amplitudes. These are determined in, e.g., the MAID analysis [100]; the connection between these helicity amplitudes and the vector form factors is given in [99]. The resonance contribution determined by  $C_5^A(0)$  (see Eq. (18) in [101]) is obtained by fitting the available pion electro-production data on an elementary target. The quality of these data is, however, not sufficient to determine all four axial form factors  $C_i^A(Q^2)$ . Already in Ref. [102] it was noticed that  $C_5^A$  gives the dominant contribution.  $C_6^A$  can be related to  $C_5^A$  by PCAC [103] and  $C_3^A$  is set to zero based on an old analysis by Adler [104], whereas  $C_4^A$  is linked to  $C_5^A$ . Based on these relations all theoretical analyses have so far only used the one axial form factor  $C_5^A(Q^2)$  with various parameterizations that usually go beyond that of a simple dipole [101, 105, 103, 106].

Both experiments also had extracted various invariant mass distributions from their data. The analysis of these invariant mass data together with the experimental  $d\sigma/dQ^2$  distributions then led the authors of [107] to conclude that probably the BNL data were too high. This has been confirmed by a reanalysis of the old data by Wilkinson et al [108] who used the QE data obtained in the same experiment for a flux calibration. After that flux recalibration the BNL data agree with the ANL data. There remains an uncertainty, however, that is connected with possible final state effects in the extraction of pion production cross sections on the nucleon from data obtained with a deuterium target [109].

*3.5.2. Background amplitudes* Theoretical descriptions of pion production can use many available data on photo- and electro-production of pions on nucleons for a check of the method [110, 111, 112, 113]. A complication in determining the form factors from comparison with data is due to background contributions that contribute to the observed cross section. For *electro*-production of pions also *t*-channel and Born-type processes provide a background to the resonance contribution. The total cross section is then given by the coherent sum of *s*-channel and *t*-channel amplitudes. Analogously, also for the case of *neutrino*-interactions there is a background contribution due to Born-type diagrams where the incoming  $W^+$  (for neutrino-induced CC pion production) interacts with the nucleon line  $WN \rightarrow N'\pi$ . The Lagrangian for this latter interaction can be obtained from effective field theory, for low energies up to about the  $\Delta$  region [107, 114, 115]. The description for the  $\Delta$  region obtained with this model is quite good, but for the higher-lying resonances one has to resort to modeling both the resonance and the background contributions. Since for higher lying resonances there is even less experimental information available all models simply use dipole parameterizations for the resonance transition form factors with the strength obtained from PCAC [107].

Significantly more involved, but also much more ambitious, is the dynamical coupled-channel model of photo-, electro- and weak pion production developed in Ref. [116] that has been applied to all resonances with invariant masses up to 2.1 GeV. In this model background and resonance contributions emerge from the same Lagrangian and thus the relative phase between resonance and background amplitudes is fixed. Furthermore, not only pion, but also other meson production channels, for example, for

the important  $2\pi$  production as well as for kaons and etas, can be predicted. It is a theoretical challenge now that these calculations give a cross section which is close to the higher-lying BNL cross sections for single pion production. Since these elementary data on the nucleon are an essential input into calculations for production on nuclei, where pion production plays a major role also for neutrino oscillation analyses this point has to be settled. New measurements on elementary targets are thus desperately needed to settle this nagging problem.

At the start of this section I have discussed that representing a coherent sum of amplitudes in a semiclassical calculation poses a problem that requires some practical approximation. In GiBUU, for example, the resonance part alone is handled by exciting nucleon resonances that are then being propagated as new particles until they decay again. The sum of the background part and the interference part is lumped together into a background term; it is assumed that pions that are due to this 'background' are produced immediately. GENIE uses instead the Rein-Sehgal model for the resonance excitation and a tuned fit to average total cross sections as background.

*3.5.3. Pion production and absorption* Pion production and pion absorption are closely linked through basic quantum mechanical constraints. This can be clearly seen for an energy regime where only the nucleon resonances are essential and DIS does not yet contribute significantly, i.e. in the energy regime of T2K and MicroBooNE. Here the resonance ( $\Delta$ ) contribution to pion production proceeds as

$$W^+ + N \rightarrow \Delta \rightarrow \pi + N' , \quad (27)$$

whereas pion absorption proceeds through the same resonance

$$\pi + N \rightarrow \Delta \quad \Rightarrow \quad \Delta + N \rightarrow N' + N'' . \quad (28)$$

In both processes the very same  $\pi N \Delta$  vertex appears, once in the  $\Delta$  production and once in its decay.

The generators GENIE, NEUT and NuWro all violate this time-reversal invariance condition by using quite different models for pion production and absorption. For example, in these standard generators the production is described by resonance excitations within the Rein-Segal model, whereas pion reabsorption is handled by a very different model, mostly the pion-absorption cascade of the Valencia group [117]. This is particularly dangerous if then – as usual in the generators – tuning parameters are introduced that allow to tune pion production and pion absorption independently from each other. This obviously introduces artificial degrees of freedom.

Only the generator GiBUU respects this connection between production and absorption of pions in the resonance region.

### 3.6. Deep inelastic scattering

Neutrino physicists have traditionally defined all reactions connected with the emission of more than 1 pion as Deep Inelastic Scattering (DIS). This is an oversimplification since

over the last 30 years the study of nucleon excitations has shown that up to invariant masses of about 2 GeV there are many resonances that also decay into 2 and even more pions; the  $2\pi$  threshold opens at about a mass of 1.5 GeV. Only above about 2 GeV the individual nucleon resonances start to overlap and the DIS regime starts. Furthermore, nucleon resonance excitations and DIS have very different  $Q^2$  dependencies such that DIS is connected with events with  $Q^2 > 1 \text{ GeV}^2$ .

The semi-inclusive cross sections for DIS can be expressed in terms of structure functions [118]. In the pQCD regime, i.e.  $Q^2 > 1 \text{ GeV}^2$ , these structure functions can be written down in terms of parton distribution functions. In regions, where pQCD does not yet provide the correct description, parameterizations of these structure functions have been obtained by fits to semi-inclusive cross section data. The high-energy event generator PYTHIA [119] is then often used to actually provide also mass- and energy-distributions of the final state. When using this framework for neutrino-nucleus reactions one is faced with the complication that the target nucleon is bound, i.e. off shell. Various schemes have been investigated to deal with this problem; it was found that these effects do play a small, but visible role at intermediate energies [120].

Also for DIS reactions electro-production data provide an excellent testing ground for generators. In particular the HERMES data, taken with a lepton beam at 28 GeV and 12 GeV incoming lepton energy on nuclear targets up to Xe [121, 122], but also the JLAB data taken by Brooks et al [123] are particularly relevant for such tests. These data have been analyzed with an early version of GiBUU [124]. This latter study also has shown that the often used prescription to forbid any interactions within a so-called 'formation-time' is unrealistic and not in agreement with the data from HERMES and the EMC experiment.

#### 4. Final state interactions

In the preceding sections I have already mentioned the importance of final state interactions (fsi), e.g. in connection with the final state potential in QE processes or in connection with pion reabsorption. These final state interactions are due to hadron-hadron interactions. They are thus independent of the electroweak nature of the initial interaction. In this section I now summarize some of the methods used in generators to describe fsi. This description can necessarily only be rather superficial since there often exist no detailed write-ups of the physics used in these generators and their algorithms. A notable exception is GiBUU for which both the physics and many details of the numerical implementation have been extensively documented [23].

Final state interactions can be split into two categories. One kind of fsi is that caused by the presence of mean field potentials which must be there not only for the initial, but also the final state. Particles then move on possibly complicated trajectories that can have an influence on observed final state angular distributions. A second kind of fsi is that which an initially produced particle experiences when it collides with other nucleons inside the target on its way out of the nucleus to the detector. In such collisions

both elastic and inelastic scattering can take place, possibly connected also with charge transfer. All the generators use a frozen density distribution for the target nucleus. The ejected particle then undergoes collisions inside that density. The probability for these collisions and the final channel in such a collision are determined by the mean free path of the particle and the cross section for the special final state relative to the total one.

One problem that one faces in this description is that the neutrino 'illuminates' the whole target nucleus and, therefore, any kicked out (nucleons) or produced (pions) particles can start their way through the nuclear target at any density. This is very different from a reaction in which an incoming particle hits a nucleus from its outside. For example,  $\pi A$  absorption data are sensitive to the overall absorption only, they do not give, however, any information on the mean free path inside the nucleus as long as their mean free path is smaller than the nuclear diameter. A significantly better check is provided by photo-production of pion data on nuclei ( $\gamma A \rightarrow \pi A^*$  since the incoming photons illuminate the whole nuclear volume, just as neutrino do. Unfortunately, no such comparisons of generator results with photo-production data are available, the notable exception being again GiBUU [111, 110]. Disregarding this fact the generator GENIE uses as basic input for its treatment of fsi a tuned model for collisions of a particle beam with one medium-heavy nucleus, such as Fe. Mass-scaling is then invoked to describe these interactions on lighter nuclei, such as C.

In the following discussion I will briefly go through some of the models used in generators||.

#### (i) Effective Models

- GENIE hA In this model the cascade is reduced to a single step in which e.g. pions are impinging on an iron nucleus and then scaled to other nuclei.
- GENIE hA 2014 uses the same oversimplification, only the  $A$ -scaling has been improved

This model, which still is the default in GENI goes back to the INTRANUKE program developed about 25 years ago; it is "simple and empirical, data-driven" in the words of the GENIE manual, but is really quite outdated. It suffers from the problem discussed above that a particle +  $A$  reaction does not describe the relevant physics of a particle being produced inside the nucleus and then cascading through it.

#### (ii) Cascade models

- GENIE hN is a "full intranuclear cascade" model, according to the manual of v. 3.0, but no details are given. Obviously pion production and absorption are treated independent from each other. Hadrons move freely, without potentials.
- NuWRo The NuWRo generator suffers from the same deficiency just discussed: detailed balance is violated since the model used for pion production is not consistent with the Oset model. Hadrons move freely, without potentials.

|| For GENIE I rely on the manual, dated March 13, 2018, to be found at <https://genie-docdb.pp.rl.ac.uk/cgi-bin/ShowDocument?docid=2>

- FLUKA [125] is a model that has been widely used for all sorts of nuclear and hadron interaction studies. It also has a neutrino option [41], but so far has not been used to analyze or reproduce neutrino data from ongoing experiments.
  - NEUT Nucleon beam scattering data are used to tune the nucleon fsi. The final state interactions of different particles, such as pions, are handled by introducing tunable multiplicative factors that are different for different physics processes. For pions the fsi were originally handled by simple attenuation factors; more modern versions of the code use the Valencia cascade for the fsi; this violates detailed balance as discussed above.
- (iii) **Transport Models** The GiBUU transport model starts the outgoing particles inside the nuclear volume and then propagates them out of the nucleus. It respects the detailed balance constraints on pion production and absorption in the resonance region. The relevant cross sections for both processes are calculated within one and the same theoretical model (see App. B1 in [23]). The pion final state interactions are then handled by a full cascade which is relativistically correct. Calculations for neutrino-nucleus reactions so far also have used the frozen configuration approximation. GiBUU does allow also to treat the target nucleons dynamically; this could become important when at high incoming energies the target nucleus is significantly disrupted.

#### 4.1. Tuning of generators

Finally, a comment is in order on tuning the generators to data. This is a widespread practice among experimentalists using neutrino generators such as GENIE and NEUT. This is well justified if the tuning consists in adjusting cross sections and potentials. These inputs to generators all carry with them some experimental uncertainties and varying them within the experimental error bars is justified. Such fits of physics parameters to data could actually help to decreasing the experimental uncertainties.

On the other hand, often also unphysical parameters are tuned. An example is the use of different momentum distributions (global vs. local Fermi gas) in describing different elementary processes or the 'brute force' change of physics input. Another example is provided by the tuning of 2p2h cross sections in the MINERvA experiment[79]. Their generator version originally started with a description of 2p2h processes taken from the Valencia model [77]. After comparing with data it was found that this 2p2h contribution is too weak and its integrated strength had to be increased by about 53% [126]. This increase was not achieved by changing coupling constant or similar physics parameters, but instead by fitting a 2d function with free parameters directly to the data.

A very recent analysis of the MINERvA pion data has shown that even allowing tuning of GENIE ingredients does not give a satisfactory fit to the data [94]. Similarly, an analysis of pion-nucleus data using the generator NEUT has shown significant discrepancies between data and generator result [93]. One may wonder, however, about

the ultimate conclusion from these studies which showed that incorrect physics models could not even be fitted to data. GiBUU, on the other hand, which contains a consistent pion production model in the resonance region, has successfully reproduced many pion data without any special tune [65, 127].

## 5. Generator results

In this section I use some results of the generator GiBUU to illustrate some properties of neutrino-nucleus interactions in different energy regimes and for different targets. I will start with semi-inclusive cross sections and then also show some more exclusive observables for the experiments T2K, MINERvA, MicroBOONE and DUNE. Some emphasis will be put on the question if the isospin-dependence of the 2p2h interactions can indeed be observed.

All results shown in this section were obtained with the 2019 version of GiBUU [22] running in the quasiparticle approximation described in Sect. 2.3.3. No special tune was used; all calculations for different incoming flux distributions and for different targets were obtained with one and the same set of input parameters 'out of the box'.

### 5.1. Comparisons with electron data

Even though the community in general agrees that checks of generators against electron data are necessary there exist very few published comparisons of generator results with such data. For NEUT there are no published comparisons available, for GENIE only very recently some comparisons have become available [128, 129] which indicate serious discrepancies with data in all of the inelastic excitation region. For NuWro only some preliminary results exist [130]. For GiBUU there is a long list of comparisons both with electron and photon data available [45, 46, 124, 131, 132, 133, 134, 135, 131, 136, 137, 138, 139, 140, 141, 142, 143, 144, 145] which cover both inclusive and semi-inclusive particle production data obtained in electro-nuclear and photo-nuclear reactions.

### 5.2. Semi-inclusive cross sections

**5.2.1. T2K** The mean beam energy at T2K is about 750 MeV so that one expects that here QE scattering and pion production through the  $\Delta$  resonance are dominant. This is indeed borne out in the semi-inclusive cross section shown in Fig. 4. While all angular bins look very similar, with a QE scattering peak at about  $T_\mu = 0.5$  GeV, the most forward bin ( $\cos(\theta) = 0.975$ ) shows a different behavior, with a long, flat shoulder out to higher  $T_\mu$ . This behavior shows up already in the individual QE and  $\Delta$  contributions shown separately in the figure. It is due to the higher energy tail in the incoming neutrino flux. In addition, also DIS starts to contribute at about  $T_\mu = 1$  GeV (not explicitly shown in the figure). Note that the 2p2h contribution is essential absent in the most forward bin. This reflects the transverse character of this reaction type in GiBUU.

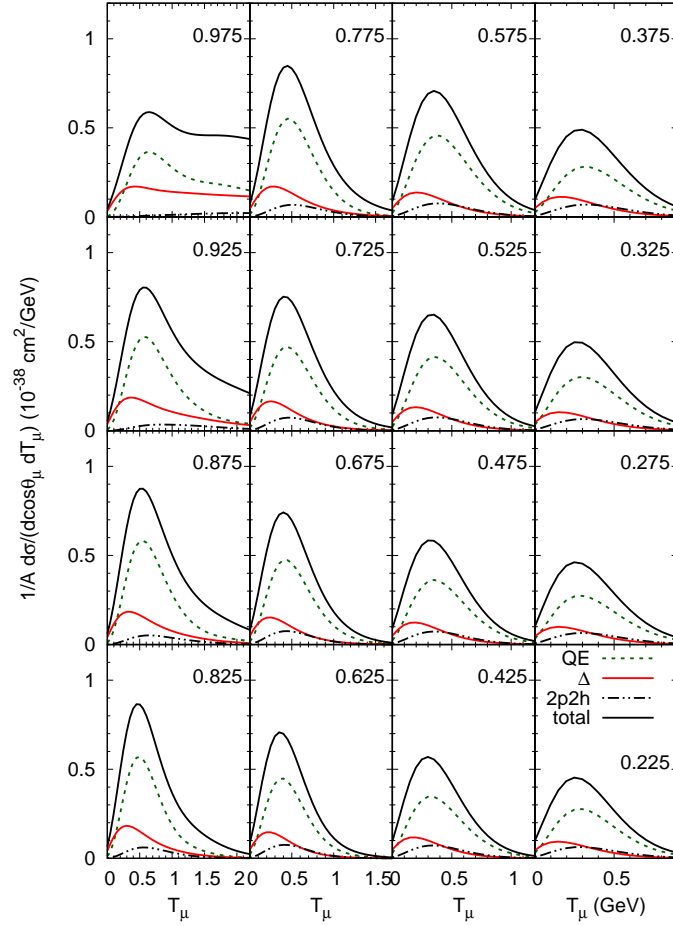


**Figure 4.** Double-differential cross section per nucleon for outgoing muons for the T2K neutrino beam hitting a  $^{12}\text{C}$  target at the near detector. The different curves depict the contributions of CCQE scattering,  $\Delta$  excitation and 2p2h processes to the cross section as a function of the outgoing muon kinetic energy, as indicated in the figure. The numbers in the upper parts of each subfigure gives the cosine of the muon scattering angle with respect to the neutrino beam. All cross sections are given per nucleon.

**5.2.2. MicroBooNE** MicroBooNE is an experiment that runs in the Booster Neutrino Beam with an  $^{40}\text{Ar}$  target. It has  $4\pi$  coverage; therefore I show in Fig. 5 the double

differential cross section over the full angular range. The forward bin centered at  $\cos(\theta) = 0.95$  is now wider than the one shown before for the T2K experiment which is narrower and centered even more forward. The flat behavior of the total cross section in the forward bin for T2K thus does not show up here in the plot of the dd distribution for MicroBooNE. Otherwise, the results are quite similar, with the exception of the 2p2h contribution that is now larger than for T2K, reflecting the non-zero isospin of the target nucleus  $^{40}\text{Ar}$  ( $\mathcal{T} = 2$ ). It will be most interesting to see if this increase in the 2p2h strength is indeed borne out by the data that are presently being taken. A verification would give direct information on the states that are excited in a neutrino-nucleus 2p2h reaction.

*5.2.3. MINERvA LE and ME* The MINERvA experiment runs at a higher energy, but with targets similar to those used in the T2K ND detector. The mean beam energy in its lower energy (LE) configuration is about 3.5 GeV so that one expects a larger contribution of resonance excitations and even DIS in this case. This can indeed be seen in the lepton semi-inclusive double-differential (dd) cross sections as a function of muon kinetic energy in various angular bins in Figs. 8. The experiment has acceptance cuts. Muons with energies below about 1.5 GeV and with angles larger than 20 degrees are not detected. These cuts are also used in the figure.

One sees that the cross sections are strongly forward peaked. In the most forward bin ( $\cos(\theta) = 0.995$ ) QE and  $\Delta$  excitation nearly completely overlap. Both together make up more than 3/4 of the total cross section in that bin. The 2p2h contribution is comparatively negligible (about 5% of the total); at the peak of the total cross section the 2p2h contribution is the smallest of all. DIS accounts for less than 10 % in the peak region of that bin, but it has a long high-energy tail¶. For muon kinetic energies above about 4 GeV the DIS contribution becomes dominant. In the next angular bin ( $\cos(\theta) = 0.985$ ) DIS accounts for nearly all of the cross section for  $T_\mu > 4$  GeV. This defines an optimal kinematical region for studies of DIS in neutrino-induced reactions.

Figure 7 gives the  $Q^2$  distribution, where  $Q^2$  here is calculated from  $Q^2 = 4E_\nu E_\mu \sin^2(\frac{\theta_\mu}{2})$ .

Since  $Q^2$  cannot directly be measured but must be reconstructed, this is a less direct observable than the dd cross sections. Nevertheless it is interesting to see that the inclusive  $Q^2$  distributions reach out to fairly large  $Q^2$  while the distribution for 0-pion events dies out at  $Q^2 \approx 1.5 \text{ GeV}^2$ . The latter reflects the fact that in 0-pion events resonance excitations and DIS, which both dominantly decay into a nucleon and pions, are suppressed. DIS events are connected with momentum transfers  $Q^2 > 1 \text{ GeV}^2$  where they contribute significantly to the inclusive cross section.

Presently, the MINERvA experiment is also running at a so-called medium energy (ME) where the flux peaks at about 5.75 GeV. If one looks at the same distributions as before now for the medium energy energy beam one sees similar shapes for the overall

¶ In GiBUU all events connected with nucleon excitations above an invariant mass of 2 GeV is identified with 'DIS'



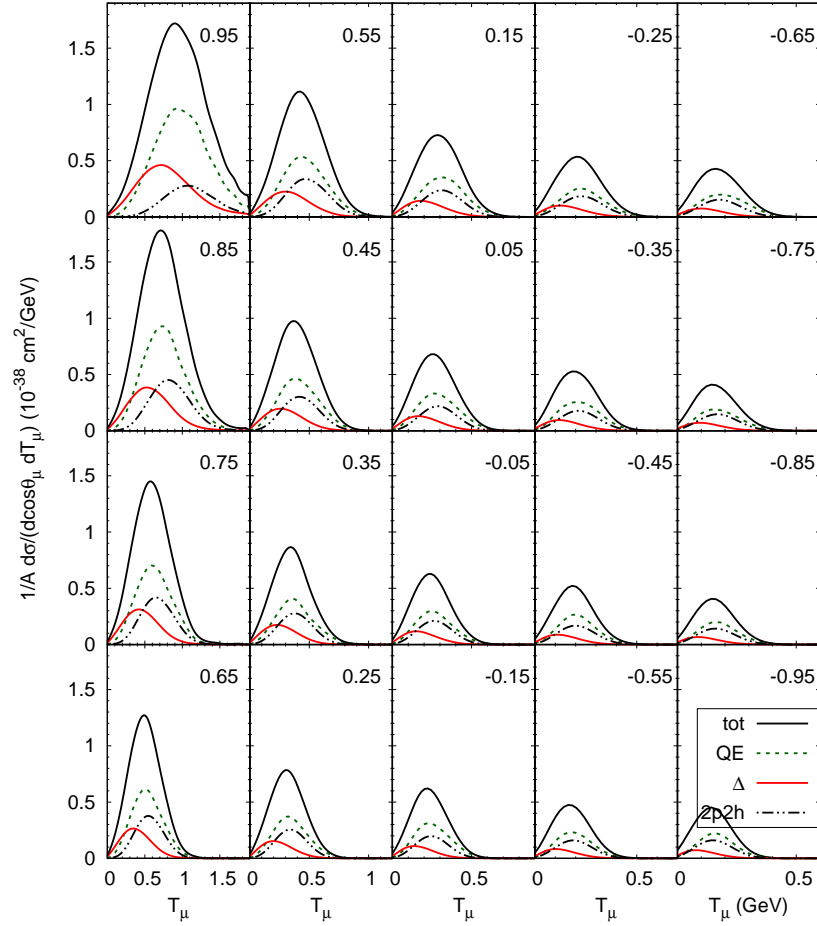


**Figure 5.** Double-differential cross section per nucleon for outgoing muons for the MicroBooNE experiment with a  $^{40}\text{Ar}$  target. The different curves depict the various contributions to the cross section as a function of the outgoing muon kinetic energy, as indicated in the figure. The numbers in the upper parts of each subfigure gives the cosine of the muon scattering angle with respect to the neutrino beam. All cross sections are given per nucleon.

cross sections. Again  $\Delta$  excitation and QE scattering give about equal contributions to the cross section at the most forward bin. In that bin ( $\cos(\theta) = 0.995$ ) the DIS contribution is larger already under the peak. It becomes dominant in the next angular

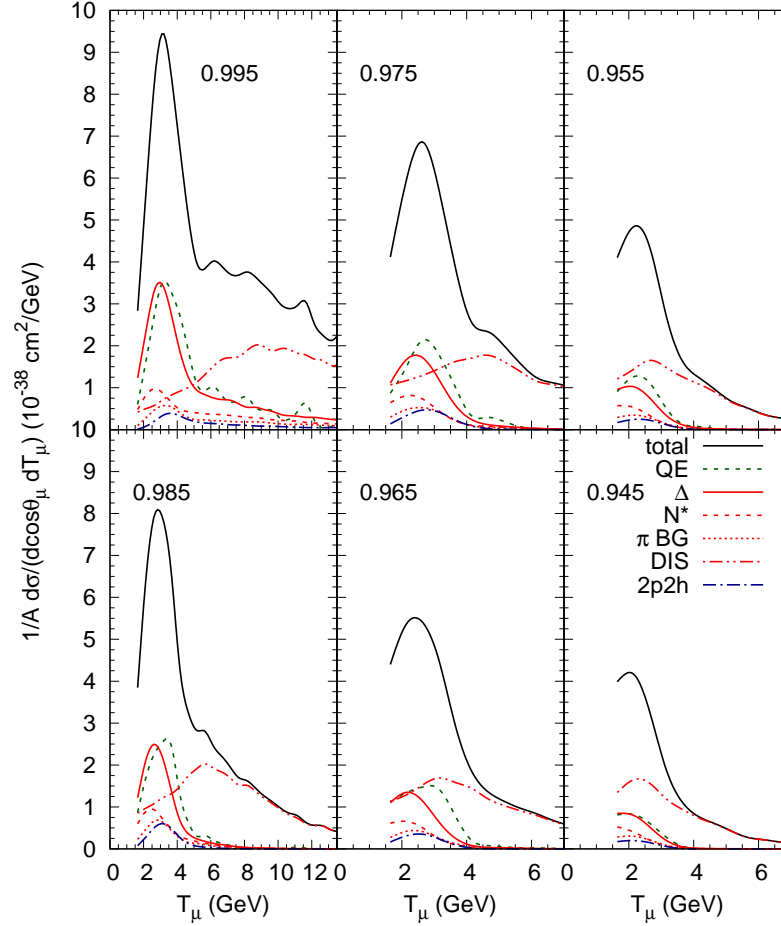


**Figure 6.** Double-differential cross section per nucleon for outgoing muons for the MINERvA lower energy neutrino beam hitting a  $^{12}\text{C}$  target. The different curves depict the various contributions to the cross section as a function of the outgoing muon kinetic energy, as indicated in the figure. The numbers in the upper parts of each subfigure gives the cosine of the muon scattering angle with respect to the neutrino beam. All cross sections are given per nucleon.

bin ( $\cos(\theta) = 0.985$ ) and from ( $\cos(\theta) = 0.975$ ) on it accounts for nearly all the cross section. Choosing only events with the outgoing muon angle  $> 10$  degrees thus enriches the DIS events significantly and should be chosen for any experimental study of that

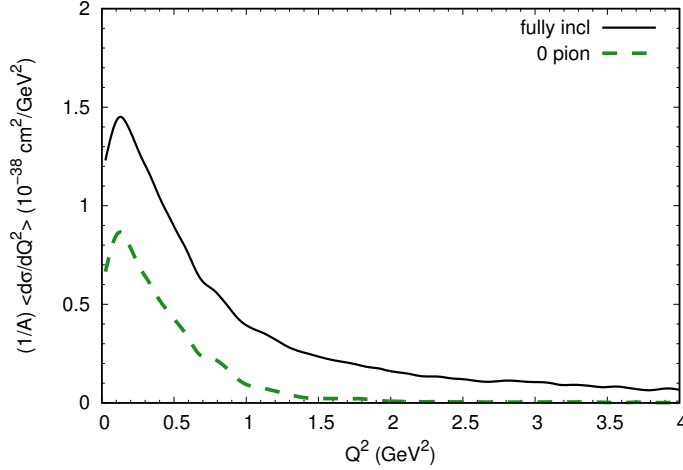
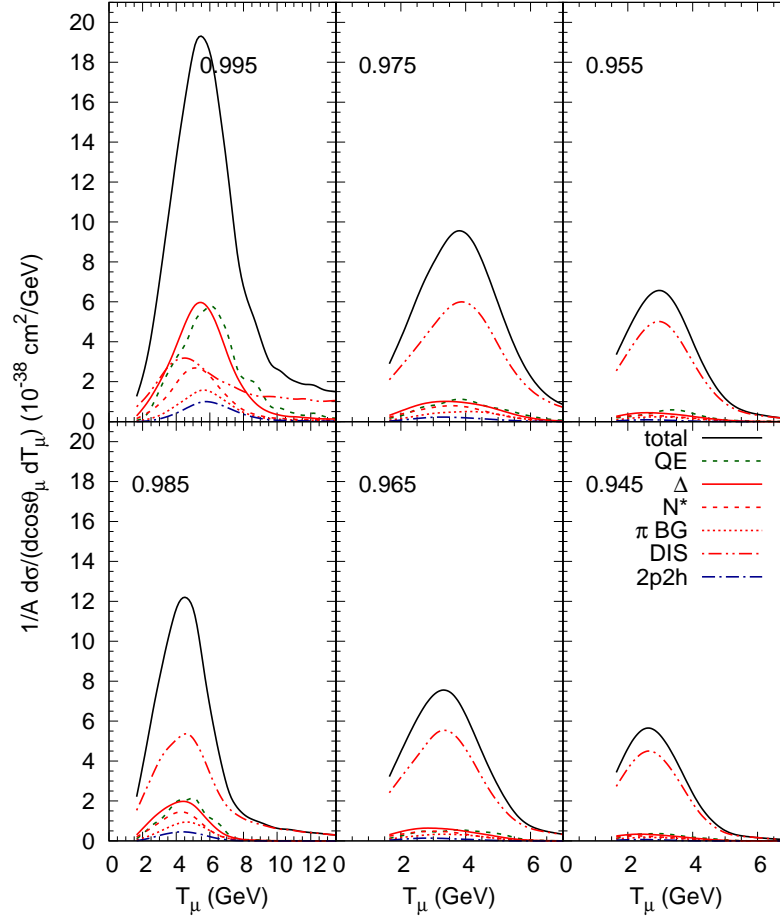


**Figure 7.**  $Q^2$  distribution per nucleon for inclusive and for 0-pion events in the MINERvA LE beam hitting a  $^{12}\text{C}$  beam.

reaction process. The  $Q^2$  distribution (Fig. 9) is similar to the one at the LE flux. Again restricting the events to those with zero outgoing pions cuts the cross section by nearly a factor 2 at small  $Q^2$  and brings the cross section down to nearly zero at  $Q^2 \approx 2.5$  GeV.

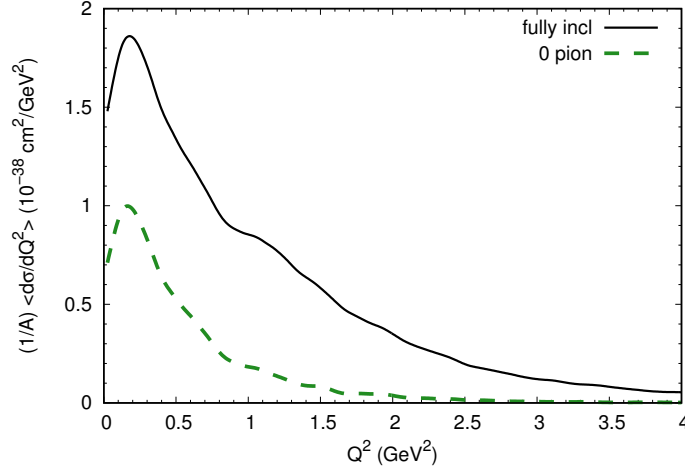
**5.2.4. ArgoNeut** The data from ArgoNeut are particularly interesting because this experiment was the first to use an Ar target in a higher energy beam. Figs. 10 and 11 show the double-differential cross section for a neutrino beam in the antineutrino mode; this flux peaks at about 6 GeV with a long, hard tail out to larger energies. It is noticeable that now even in the most forward bin ( $\cos(\theta) = 0.995$ ) the largest contribution now comes from DIS, which contributes about a factor of three more than QE and  $\Delta$  processes. This is due to the fact that DIS cross sections depend approximately linearly on the incoming neutrino energy and the ArgoNeut flux has significant strength also at higher energies. These Ar data could in principle serve as a testing ground for the isospin dependence of the 2p2h component. However, this component is so small even for  $\mathcal{T} = 2$ , compared to the dominant DIS contribution, so that there is hardly any sensitivity to its strength.

Fig. 11 gives the muon momentum spectrum for the same experiment. Shown are results for a calculation with  $\mathcal{T} = 2$ , but a calculation with  $\mathcal{T} = 0$  gives nearly the same curve. Also shown is the spectrum for 0-pion events. This cross section is quite flat and significantly smaller than the inclusive one. The latter feature is due to the dominance of DIS in the fully inclusive cross section and to the fact that DIS events nearly always lead to pions in the final state.



**Figure 8.** Same as Fig. 6 for the MINERvA medium energy neutrino beam.

*5.2.5. DUNE* Finally we discuss here the semi-inclusive cross section for the DUNE near detector (ND). DUNE will work with a neutrino flux similar to the MINERvA LE flux, but with  $^{40}\text{Ar}$  as a target. On the one hand, we thus expect a very similar behavior as for MINERvA, in particular a strong forward peaking of the cross section. On the other hand, the isospin of  $^{40}\text{Ar}$  is  $\mathcal{T} = 2$  and it will be interesting to look for any observable consequences of that isospin change. All calculations for the DUNE ND were performed with the flux from [147].



**Figure 9.**  $Q^2$  distribution per nucleon for inclusive and for 0-pion events in the MINERvA ME beam hitting a  $^{12}\text{C}$  target.

That the dd cross section is indeed quite similar to the one obtained for the MINERvA LE run can indeed be seen in Fig. 15 of Ref. [46]. We show, therefore, now only the most forward angles in Fig. 12. Most noticeable is the significantly larger (than in the MINERvA LE run) contribution of 2p2h excitations that comes about because the target nucleus Ar has  $\mathcal{T} = 2$  whereas in the MINERvA experiment the target is C with  $\mathcal{T} = 0$ . This difference leads to an enhancement of the 2p2h cross section by a factor 3 relative to the one on C. DIS is not as large as it is in the ArgoNeut experiment because the incoming flux does not have the sizeable high energy tail that the ArgoNEUT flux had.

### 5.3. Semi-inclusive cross sections for hadrons

From the preceding discussions it is clear that already the inclusive cross sections are made up of various quite different reaction mechanisms, the most important ones being QE scattering and pion production (through resonances and DIS). This is already a challenge even for theories that describe inclusive cross sections, such as GFMC and SUSY inspired models, since they usually cannot handle the elastic and the inelastic processes with a comparable accuracy.

In this subsection I will now illustrate some features of semi-inclusive cross sections for processes with outgoing hadrons in the DUNE Near Detector (ND). These can, for example, be spectra of certain given particles while an integration over all other degrees of freedom is performed. This is the actual strength of generators such as GiBUU which yield information about the complete final state.

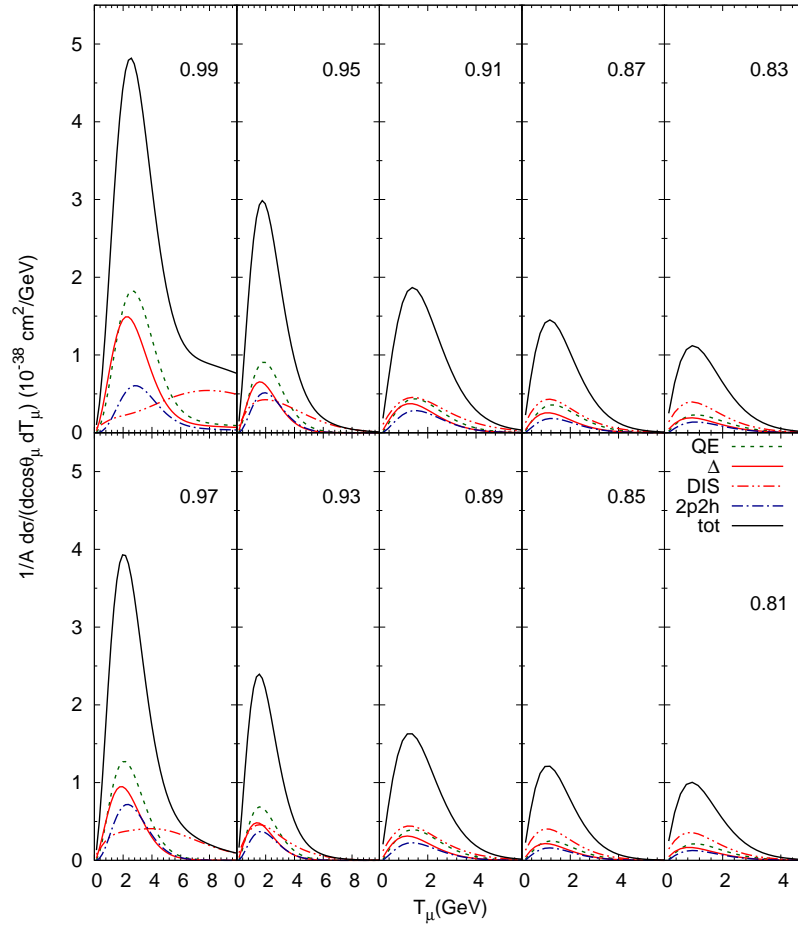


**Figure 10.** Lepton semi-inclusive double differential cross section in the forward region for the ArgoNEUT experiment. The numbers in each bin give the central  $\cos(\theta)$  value of the angular bin. Some contributions from different reaction mechanisms are indicated in the figure.

*5.3.1. Transparency* Before coming to the DUNE cross sections for outgoing nucleons it is interesting to look at a comparison with the transparency of nuclei for outgoing nucleons was measured in electron-induced reactions for different targets and over a wide range of momentum-transfer  $Q^2$ . The comparison of GiBUU results, obtained already in 2001, with the data is shown in Fig. 13. The agreement is obviously quite good.

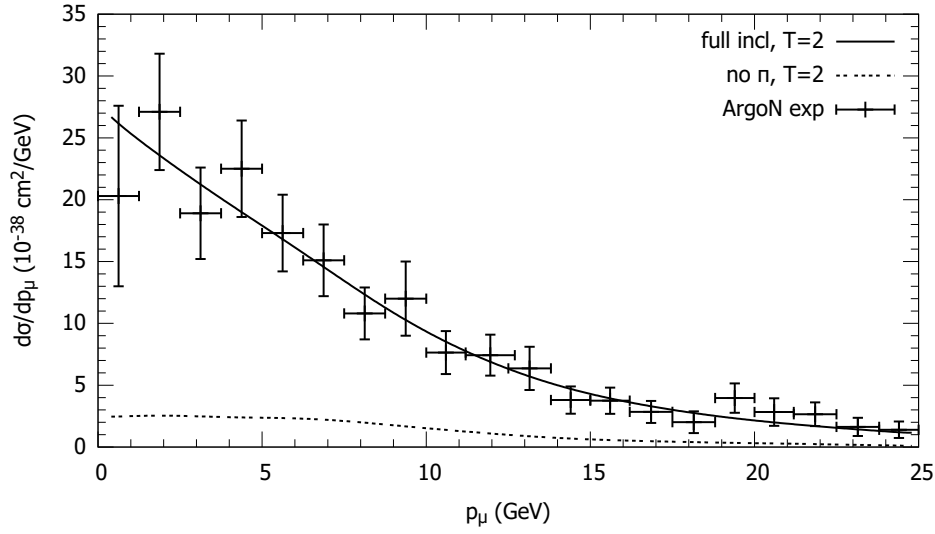


**Figure 11.** Semi-inclusive muon momentum spectrum for the ArgoNEUT experiment. Data are from [146].

The structures in these curves are mostly explained by experimental constraints on the intervals over which the experimental transparencies were determined [151].

**5.3.2. Particle spectra** Fig. 14 shows the kinetic energy spectra of protons and neutrons expected for the DUNE experiment. Plotted are both the spectra for events with one and only one outgoing nucleon and those for multi-p or multi-n events. While the former are small and quite flat as a function of nucleon kinetic energy the multi-nucleon events exhibit a steep rise in their spectra below about 0.3 GeV<sup>+</sup>. This rise is due to final state interactions: While at the end of the first, initial neutrino-nucleus interaction there may be only one nucleon outgoing, its collisions with other nucleons causes an 'avalanche' of nucleons. Energy conservation then requires that all these secondary particles carry lower energies. This steep rise also implies that caution has to be taken when a calorimetric energy reconstruction is performed. Typically, the detectors have a lower detection threshold of about 50 MeV [152]. This means that a large part of the nucleon ejection cross section is not visible. This is even more so in detectors that do not see neutrons in the outgoing state.

The following two figures 15 and 16 give the pion kinetic energy and angular distributions.

The pion spectra show the typical behavior known from lower energies with a strong peak at about 0.1 GeV and a flattening around 0.25 GeV; the latter is due to pion reabsorption through the  $\Delta$  resonance. As expected for a neutrino beam  $\pi^+$  production dominates, but  $\pi^0$  is close by and even  $\pi^-$  amounts to about 1/2 of  $\pi^+$ . The

<sup>+</sup> Kinetic energy below about 30 MeV cannot be trusted in a semiclassical theory because of general quantum-mechanical effects becoming essential.

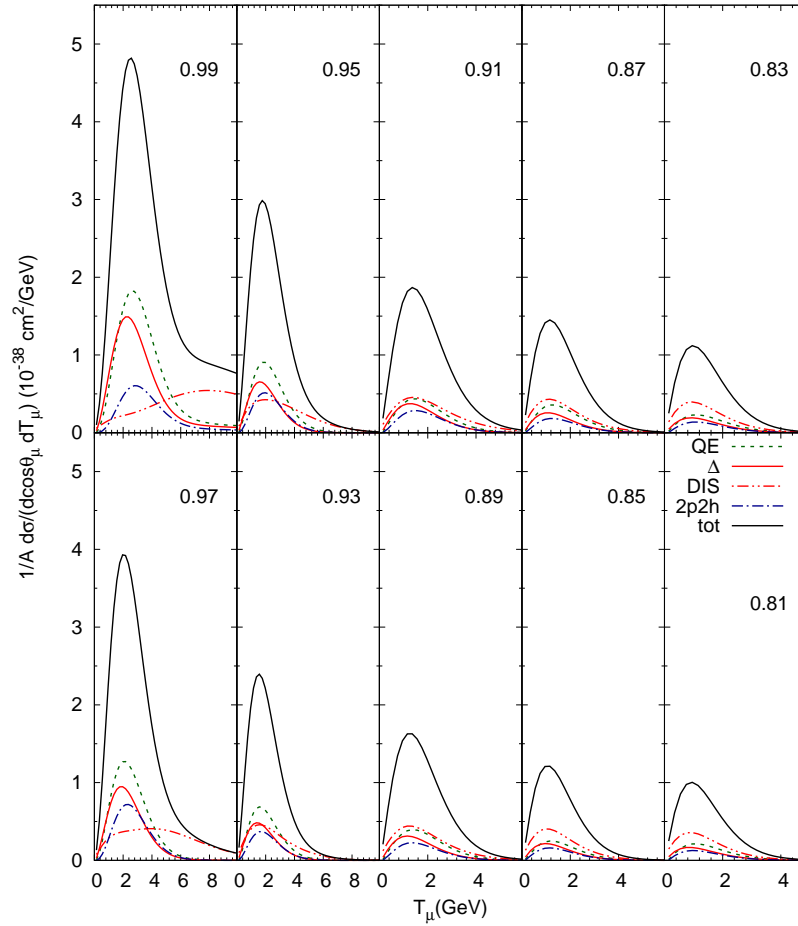


**Figure 12.** Same as Fig. 6 for the DUNE near detector in the 2017 flux.

figures also show nicely that – because of the strong DIS component – the multi-pion cross sections are much larger than the single-pion ones. All cross sections are forward peaked. Earlier theoretical studies have shown that pions with kinetic energies below about 0.03 GeV cannot reliably be described by semiclassical methods, but require a quantum-mechanical treatment [136]. The DUNE experiment will have a threshold of about 100 MeV kinetic energy [152]. This is just about where the peak of the cross section is located. Thus, the detector cuts out a nonnegligible part of the cross section.



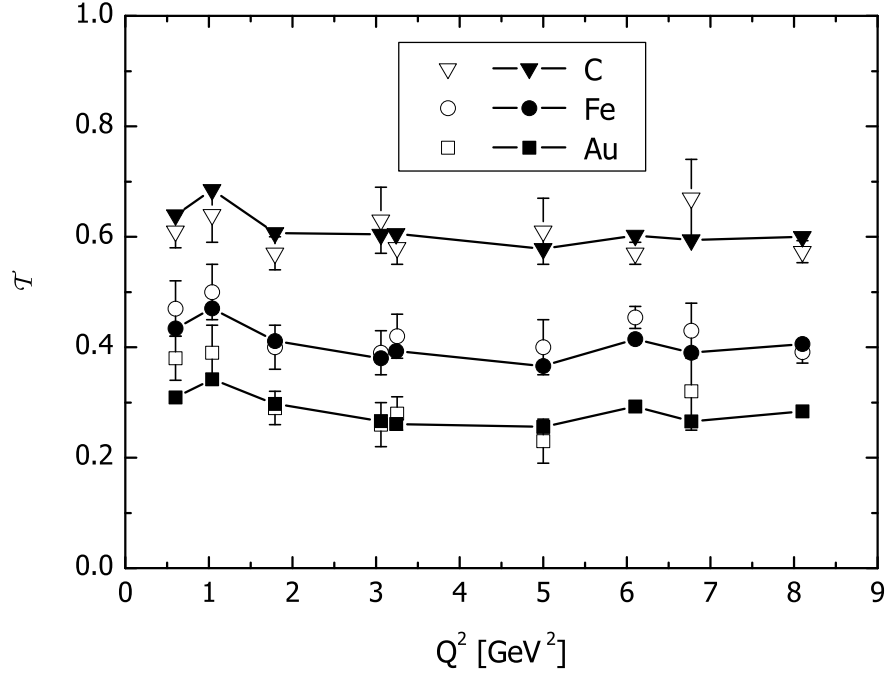


**Figure 13.** Transparency ratio for C, Fe and PB compared to data (open symbols) from JLAB [148, 149] and SLAC [150]. The full symbols represent the GiBUU results. Taken from [133, 151].

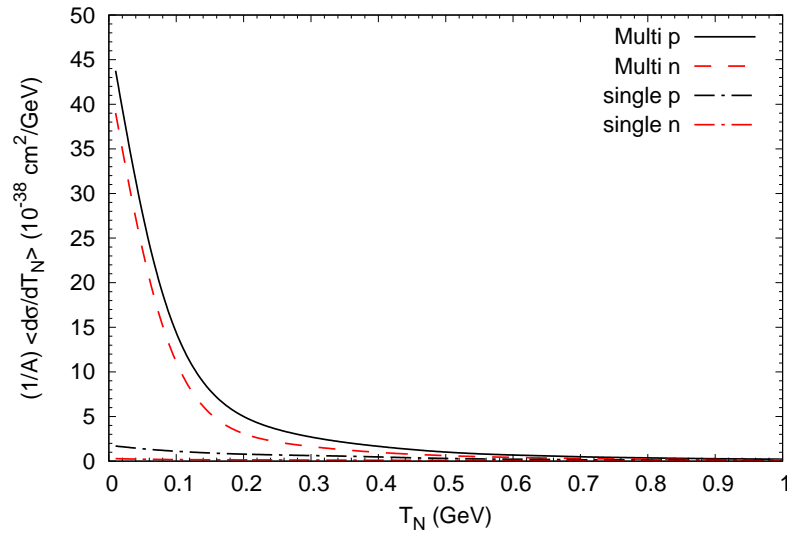


**Figure 14.** Kinetic energy spectra for protons and neutrons in the DUNE ND. Shown are results both for single and for multinucleon events.

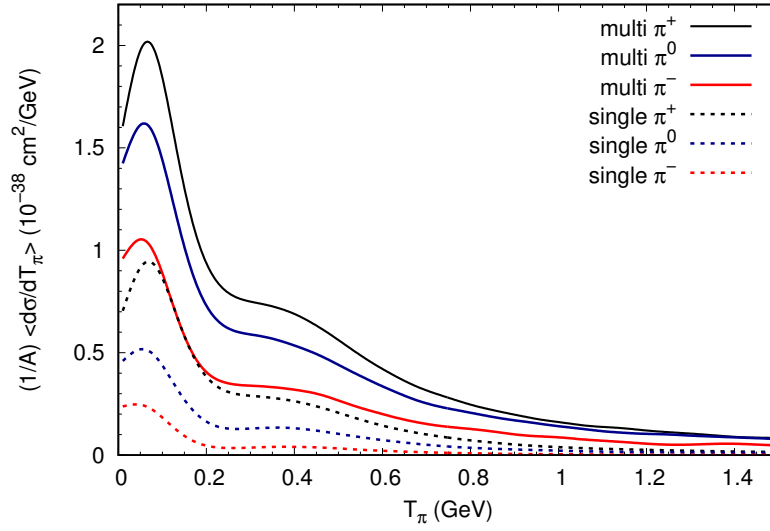


**Figure 15.** Kinetic energy spectra of incoherently produced pions for all charges in the DUNE ND. Shown are the cross sections both for the single and the multi-meson events.

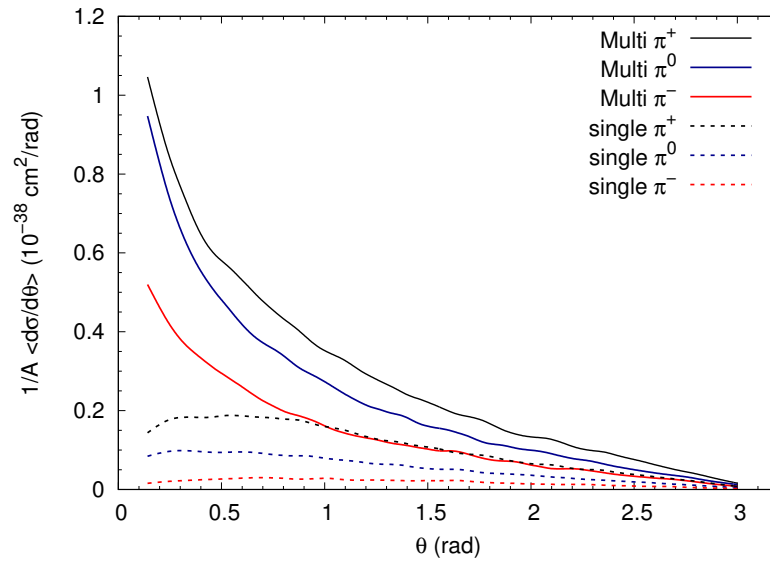


**Figure 16.** Angular distribution of incoherently produced pions of all charges both for single- and for multi-meson events in the DUNE ND.

Fig. 17 gives spectra for strange baryons. In this case single and multiple production cross sections lie on top of each other. This just reflects the lower probability (and

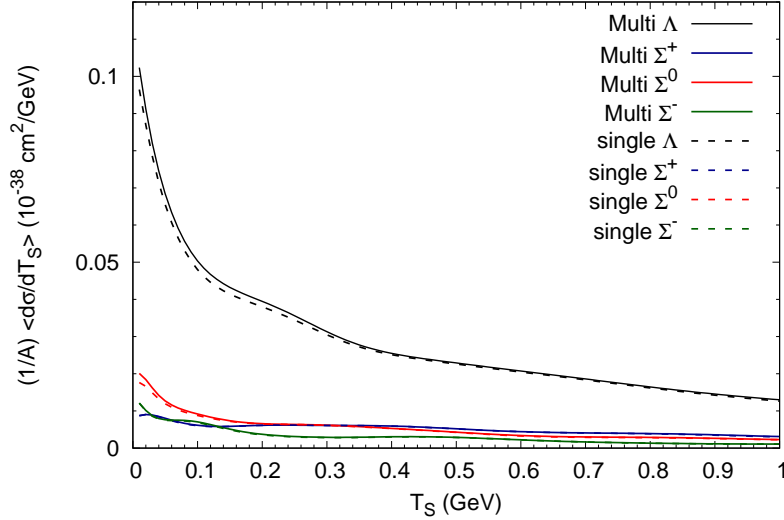


**Figure 17.** Spectra of strange baryons. Shown are both the spectra for multi-strange and for single-strange events in the DUNE ND.

higher thresholds) for strangeness production. Strangeness is produced mainly through DIS processes, often in connection with other mesons. It is seen that  $\Lambda$  production prevails. The increase of the spectrum is reminiscent of that observed above in the nucleon spectra. Indeed, the origin of that rise is again to be found in the fsi where the produced  $\Lambda$  collides with the target nucleons and thereby loses energy.

The same is true for strange meson production. There only  $K^+$  and  $K^0$  play any essential role; all the other flavors are much lower.

## 6. Summary and Conclusion

Generators are essential tools that make nuclear theory directly applicable to the description of neutrino-nucleus reactions and to the extraction of neutrino mixing parameters, the mass hierarchy and a possibly CP violating phase  $\delta_{CP}$  from long baseline oscillation experiments. If the agreement with neutrino-nucleus reaction data is good then these generators could be relied on to do the 'backwards computation' necessary to determine the incoming neutrino energy in a broad-band oscillation experiment. In view of the importance of generators for neutrino long-baseline experiments it is surprising to see that often these generators are being used by experimenters in a 'black box mode' without much knowledge about their inner workings. This information is indeed hard to come by since none of the generators GENIE, NEUT or NuWro come together with a detailed and comprehensive documentation about their physics contents and their

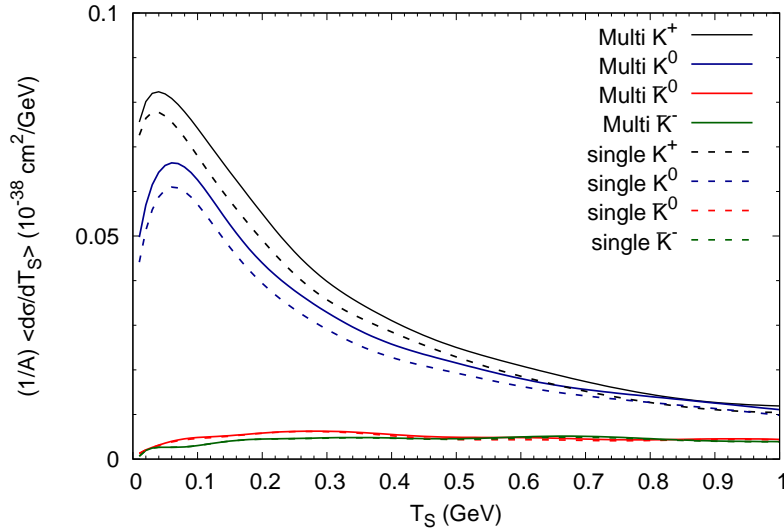


**Figure 18.** Spectra of strange mesons, both for single and for multi-meson events in the DUNE ND.

algorithms used \*. For cases where there is some text, e.g. for the treatment of fsi, the discussion is superficial. The reason is probably that the generators often incorporate quite old code fragments and methods for which the basic knowledge and the original authors are no longer available. This is different for GiBUU which represents a consistent framework of theory and code, is well documented and most of its primary authors are still active in the field.

For a test of generators besides neutrino data themselves also data from electro-nuclear or photo-nuclear reactions are useful and necessary. Their initial reactions are identical with the vector part of neutrino-induced reactions and the final state interactions are the same if the incoming kinematics (energy- and momentum-transfer) are identical. Checking generators against electron or photon data is thus an indispensable requirement. So far, only a few generators can actually be used to describe photonuclear interactions. There are no published results from NEUT or NuWro available for such reactions and the results obtained with GENIE are quite unsatisfactory for energy transfers beyond the QE peak [128]. Checks with GiBUU can be found in Refs. [46, 65, 45]. Agreement with such data is a necessary prerequisite for any generator, but it is not sufficient since all these electron data were semi-inclusive ones. In addition, electro-nuclear pion [144] and  $\rho$  [140] production data could be used for a further check, as well as the many data from photonuclear pion production on nuclei [111, 110, 154, 155].

\* For GENIE even the latest manual of version 3 [153] often contains only headers, followed by empty pages.

In 2017 a group of physicists interested in the interplay of experimental and theoretical neutrino-nucleus physics published the following list of steps needed to improve neutrino generators [156]:

- (i) The development of a unified model of nuclear structure giving the initial kinematics and dynamics of nucleons bound in the nucleus.
- (ii) Modeling neutrino-bound-nucleon cross sections not only at the lepton semi-inclusive cross section level, but also in the full phase space for all the exclusive channels that are kinematically allowed.
- (iii) Improving our understanding of the role played by nucleon-nucleon correlations in interactions and implementing this understanding in MC generators, in order to avoid double counting.
- (iv) Improving models of final state interactions, which may call for further experimental input from other communities such as pion-nucleus scattering.
- (v) Expressing these improvements of the nuclear model in terms that can be successfully incorporated in the simulation of neutrino events by neutrino event generators.

In this article I have discussed that all of these points are indeed quite relevant. They are based on the shortcomings of most generators used by experimenters.

However, contrary to the impression one could have gotten from the discussions in Ref. [156] many of the points on the 'to-do list' there have actually been solved about 20 years ago. The solutions have found their way into the practical implementation in GiBUU.

I therefore now add some comments to the points above:

- (i) In contrast to all the other presently used generators only GiBUU does have the target nucleons bound in the nucleus. In its present version the phase-space distribution of these particles is semi-classical (local Thomas-Fermi gas in a mean field potential), but this initial state could be replaced by any more refined model, e.g. from nuclear many-body theory. However, the agreement with data reached already with the present model indicates that neutrino data are not very sensitive to details of the phase-space distributions. Probably this is so because the smearing over incoming energies, necessarily present in all neutrino experiments, smears out all quantum-mechanical phases.
- (ii) Generators have to provide this information on the final state and indeed all the actual generators do that; models built for lepton semi-inclusive cross sections, such as the GFMC calculations and the SUSY model calculations, cannot give that information.
- (iii) There is so far no indication for the presence of nucleon-nucleon correlations in any neutrino data. In electron experiments such correlations show up in quite exclusive reactions that fix energy and momentum transfer in reactions restricted

to one or two outgoing nucleons. Such exclusivity cannot be achieved in neutrino experiments, simply because of the broad energy distribution in the incoming beam which naturally also leads to a broad smearing over energy transfers.

- (iv) Final state interactions indeed have to be checked against data obtained in other experiments. Pion-nucleus data have indeed been used for generator checks; equally essential are particle production data from pA experiments. As discussed earlier, however, more stringent would be checks against photonuclear data since photons populate the whole nucleus whereas incoming pions suffer strong initial state interactions.
- (v) This is not a future program: all of these points are implemented in GiBUU.

### 6.1. Future developments

The ongoing and planned long-baseline neutrino experiments all strive for a precision-dominated determination of neutrino mixing parameters. These parameter can be obtained from the experimental observations only by means of a generator which has to be as up-to-date as the experimental hardware is. One cannot stress this point strongly enough: without a reliable state-of-the-art generator the experiments cannot reach their goals. It is thus time to combine scientific expertise from nuclear theory with resources mainly from the high-energy experimental community to construct a new generator which could be built on the experience reached with GiBUU, but also some of the QGP generators.

This new generator has to fulfill the following physics requirements

- Foremost, it has to be built on consistent nuclear theory, with one and the same ground state for all reaction processes. This requirement removes artificial and unphysical tuning degrees of freedom.
- It has to include potentials, both nuclear and Coulomb, from the outset. The most obvious feature of nuclei is that they are bound; generators should respect that in the preparation of the ground state. The potentials are well determined from other nuclear physics experiments; there is then no more freedom to introduce artificial binding energy parameters. Potentials will necessarily increase the computing times; this is the (small) price one has to pay for a realistic nuclear physics scenario.
- The starting point for any such generators should be transport theory. Transport theory is no longer some esoteric theoretical 'dream', but it is well established in other fields of physics as well as in nuclear physics where all the top-level experiments searching for the quark-gluon plasma (QGP) at RHIC and LHC use generators built on transport theory.
- If sophisticated spectral functions of bound nucleons actually become essential for the description of neutrino-nucleus reactions then modern transport theory provides the only consistent method to actually perform the off-shell transport necessary to bring nucleons back to their mass-shell once they leave the nucleus.

The implementation of off-shell transport in actual codes is one of the major achievements of transport theory during the last 20 years [23, 157]. It has found its way into the transport codes used by the QGP community.

From a more practical point of view any new generator should have the following properties in addition

- The generators GENIE and NEUT contain important parts which deal with the complications caused by the broad neutrino beam and the extended target sizes; both are features not present in nuclear physics experiments. These parts of the codes are essential and should be taken over into any new generator.
- The new generator should allow for easy variations of essential parameters. Elementary cross sections are an essential input into any generator and these cross sections carry experimental uncertainties. It, therefore, must be possible to vary them within their uncertainties to see the effect on the final oscillation parameters. To be distinguished from that must be the tuning of unphysical or redundant parameters which can, for example, appear when different subprocesses are described by very different theories and general principles such as time-reversal invariance are not respected.
- The new generator must be well-documented, both in its physics and its algorithms. In addition to a well-structured complete documentation a thorough comment structure in the code is necessary. After all, the neutrino generator would have to be used over the next 20 years, most probably also by physicists who were not involved in the writing of the original code. Maintenance of the code is then only possible, if documentation and comment structure are available.
- The code also must have a modular structure that allows easier modification if new theories or algorithms become available. The individual modules must respect the intrinsic connections between different processes, such as pion production and absorption. A 'platform model' in which various different groups provide alternative descriptions of individual processes may work for the technical problems such as determining detector efficiencies. It will not work for a theoretical understanding of data and for the ultimate task of extracting the relevant neutrino properties from long-baseline experiments. For these latter problems there has to be some supervisory structure that guarantees that the various processes are described on a consistent basis.

Any such new generator has to be checked against data not only from electro-nuclear experiments, but also from neutrino-nucleus interaction experiments. Since generators are used in the experiment for a determination of detector efficiencies. There is, therefore, the danger of a 'logical loop' in which a generator is first used to get the data points and then is used again to compare the data with. This is now common practice in experimental groups. Instead, a 'nuclear physics model' should be implemented; there systems such as GEANT are used to determine purely experimental properties, such as efficiencies and threshold, but the final comparison of data takes place with 'real theory'.

Any future, newly built neutrino generator will have to be tested against data obtained nowadays in experiments such as MINERvA or the ND experiments in T2K or NOvA. This test will be difficult if the published data depend on generator X version y.z for which no documentation exists. Care must, therefore, be taken that the data contain as little 'generator contamination' as possible. This is, for example, not the case if cuts on incoming neutrino energies or on invariant masses are imposed on the published data since such cuts can only be imposed by means of a generator.

## 7. Acknowledgements

I gratefully acknowledge many extremely helpful and productive discussions with Kai Gallmeister, both about the physics and the inner workings of GiBUU. I am also indebted to some of my experimental colleagues for explaining to me details of data and experiments. Here, Debbie Harris, Xianguo Lu and Kevin McFarland have been invaluable discussion partners.

## References

- [1] Boffi S, Giusti C and Pacati F 1993 *Phys.Rept.* **226** 1–101
- [2] Benhar O, Day D and Sick I 2008 *Rev. Mod. Phys.* **80** 189–224 (*Preprint nucl-ex/0603029*)
- [3] Bianchi N 2007 *Nucl. Phys.* **A782** 150–157
- [4] Dekker M, Brussaard P and Tjon J 1991 *Phys.Lett.* **B266** 249–254
- [5] Benhar O, Fabrocini A, Fantoni S and Sick I 1994 *Nucl.Phys.* **A579** 493–517
- [6] Ciofi degli Atti C and Simula S 1996 *Phys. Rev.* **C53** 1689 (*Preprint nucl-th/9507024*)
- [7] Alvioli M, Ciofi degli Atti C, Mezzetti C B, Palli V, Scopetta S, Kaptari L P and Morita H 2008 *AIP Conf. Proc.* **1056** 307–314 (*Preprint 0807.0351*)
- [8] Radici M, Dickhoff W H and Stoddard E R 2002 *Phys. Rev.* **C66** 014613 (*Preprint nucl-th/0203033*)
- [9] Hen O, Miller G A, Piasetzky E and Weinstein L B 2017 *Rev. Mod. Phys.* **89** 045002 (*Preprint 1611.09748*)
- [10] Bernard V, Elouadrhiri L and Meissner U 2002 *J.Phys.G* **G28** R1–R35 (*Preprint hep-ph/0107088*)
- [11] Smith R and Moniz E 1972 *Nucl.Phys.* **B43** 605
- [12] Llewellyn Smith C H 1972 *Phys. Rept.* **3** 261–379
- [13] Kolbe E, Thielemann F K, Langanke K and Vogel P 1995 *Phys. Rev.* **C52** 3437–3441
- [14] Nieves J, Amaro J E and Valverde M 2004 *Phys.Rev.C* **70** 055503 (*Preprint nucl-th/0408005*)
- [15] Pandey V, Jachowicz N, Van Cuyck T, Ryckebusch J and Martini M 2015 *Phys. Rev.* **C92** 024606 (*Preprint 1412.4624*)
- [16] Lovato A, Gandolfi S, Carlson J, Lusk E, Pieper S C and Schiavilla R 2018 *Phys. Rev.* **C97** 022502 (*Preprint 1711.02047*)
- [17] Mosel U 2016 *Ann. Rev. Nucl. Part. Sci.* **66** 171–195 (*Preprint 1602.00696*)
- [18] <http://www.dunescience.org/>
- [19] <http://t2k-experiment.org>
- [20] <https://novaexperiment.fnal.gov/>
- [21] Lalakulich O, Mosel U and Gallmeister K 2012 *Phys.Rev.* **C86** 054606 (*Preprint 1208.3678*)
- [22] <http://gibuu.hepforge.org>
- [23] Buss O, Gaitanos T, Gallmeister K, van Hees H, Kaskulov M *et al.* 2012 *Phys.Rept.* **512** 1–124 (*Preprint 1106.1344*)



- [24] Coloma P and Huber P 2013 *Phys.Rev.Lett.* **111** 221802 (*Preprint* 1307.1243)
- [25] Ankowski A M, Benhar O, Coloma P, Huber P, Jen C M, Mariani C, Meloni D and Vagnoni E 2015 *Phys. Rev.* **D92** 073014 (*Preprint* 1507.08560)
- [26] Gallagher H and Hayato Y (Particle Data Group) 2018 *Phys. Rev.* **D98** 030001,557
- [27] Hayato Y 2002 *Nucl.Phys.Proc.Suppl.* **112** 171–176
- [28] <http://www.genie-mc.org/>
- [29] Andreopoulos C, Bell A, Bhattacharya D, Cavanna F, Dobson J *et al.* 2010 *Nucl.Instrum.Meth.* **A614** 87–104 (*Preprint* 0905.2517)
- [30] Golan T, Sobczyk J T and Zmuda J 2012 *Nucl. Phys. Proc. Suppl.* **229-232** 499
- [31] Katori T and Martini M 2018 *J. Phys.* **G45** 013001 (*Preprint* 1611.07770)
- [32] Conrad J M, Shaevitz M H and Bolton T 1998 *Rev. Mod. Phys.* **70** 1341–1392 (*Preprint* hep-ex/9707015)
- [33] Gallagher H, Garvey G and Zeller G 2011 *Ann.Rev.Nucl.Part.Sci.* **61** 355–378
- [34] Formaggio J and Zeller G 2012 *Rev.Mod.Phys.* **84** 1307 (*Preprint* 1305.7513)
- [35] Kadanoff L and Baym G 1962 *Quantum statistical mechanics* (New York: Benjamin)
- [36] Danielewicz P 1984 *Annals Phys.* **152** 239–304
- [37] Danielewicz P 1984 *Annals Phys.* **152** 305–326
- [38] Benhar O, Fabrocini A and Fantoni S 1992 *Nucl. Phys.* **A550** 201–222
- [39] Botermans W and Malfliet R 1990 *Phys.Rept.* **198** 115–194
- [40] Lang A B H C W M U R H G and Weber K 1993 *J.Comp.Phys.* **106** 391–396
- [41] Battistoni G, Sala P R, Lantz M, Ferrari A and Smirnov G 2009 *Acta Phys. Polon.* **B40** 2491–2505
- [42] Cooper E D, Hama S, Clark B C and Mercer R L 1993 *Phys. Rev.* **C47** 297–311
- [43] González-Jiménez R, Megias G D, Barbaro M B, Caballero J A and Donnelly T W 2014 *Phys. Rev.* **C90** 035501 (*Preprint* 1407.8346)
- [44] Welke G, Prakash M, Kuo T, Das Gupta S and Gale C 1988 *Phys.Rev.* **C38** 2101–2107
- [45] Mosel U and Gallmeister K 2018 (*Preprint* 1811.10637)
- [46] Gallmeister K, Mosel U and Weil J 2016 *Phys. Rev.* **C94** 035502 (*Preprint* 1605.09391)
- [47] Nieves J, Simo I and Vacas M 2012 *Phys.Lett.* **B707** 72–75 (*Preprint* 1106.5374)
- [48] Pandey V, Jachowicz N, Martini M, González-Jiménez R, Ryckebusch J, Van Cuyck T and Van Dessel N 2016 *Phys. Rev.* **C94** 054609 (*Preprint* 1607.01216)
- [49] Nieves J and Sobczyk J E 2017 *Annals Phys.* **383** 455–496 (*Preprint* 1701.03628)
- [50] Van Dessel N, Jachowicz N, González-Jiménez R, Pandey V and Van Cuyck T 2018 *Phys. Rev.* **C97** 044616 (*Preprint* 1704.07817)
- [51] Alvarez-Ruso L, Hayato Y and Nieves J 2014 *New J.Phys.* **16** 075015 (*Preprint* 1403.2673)
- [52] Leitner T and Mosel U 2010 *Phys.Rev.C* **81** 064614 (*Preprint* 1004.4433)
- [53] Akimov D *et al.* (COHERENT) 2017 *Science* **357** 1123–1126 (*Preprint* 1708.01294)
- [54] Alvarez-Ruso L 2011 *AIP Conf. Proc.* **1405** 140–145
- [55] Leitner T, Mosel U and Winkelmann S 2009 *Phys.Rev.* **C79** 057601 (*Preprint* 0901.2837)
- [56] Peters W, Lenske H and Mosel U 1998 *Nucl. Phys.* **A640** 89–113 (*Preprint* nucl-th/9803009)
- [57] Krusche B, Ahrens J, Beck R, Kamalov S, Metag V, Owens R O and Stroher H 2002 *Phys. Lett.* **B526** 287–294 (*Preprint* nucl-ex/0304006)
- [58] Hernandez E, Nieves J and Vicente-Vacas M 2009 *Phys.Rev.* **D80** 013003 (*Preprint* 0903.5285)
- [59] Day D B, McCarthy J S, Donnelly T W and Sick I 1990 *Ann. Rev. Nucl. Part. Sci.* **40** 357–410
- [60] Caballero J A, Barbaro M B, Antonov A N, Ivanov M V and Donnelly T W 2010 *Phys. Rev.* **C81** 055502 (*Preprint* 1004.4065)
- [61] Antonov A N, Ivanov M V, Gaidarov M K, de Guerra E M, Caballero J A, Barbaro M B, Udias J M and Sarriguren P 2006 *Phys. Rev.* **C74** 054603 (*Preprint* nucl-th/0609056)
- [62] Megias G D, Barbaro M B and Caballero J A 2018 (*Preprint* 1807.10532)
- [63] Carlson J, Gandolfi S, Pederiva F, Pieper S C, Schiavilla R, Schmidt K E and Wiringa R B 2015 *Rev. Mod. Phys.* **87** 1067 (*Preprint* 1412.3081)
- [64] Lovato A, Gandolfi S, Carlson J, Pieper S C and Schiavilla R 2014 *Phys.Rev.Lett.* **112** 182502

- (Preprint 1401.2605)
- [65] Mosel U and Gallmeister K 2018 *Phys. Rev.* **C97** 045501 (Preprint 1712.07134)
  - [66] Bodek A 2018 (Preprint 1801.07975)
  - [67] Rosenfelder R 1978 *Phys. Lett.* **B79** 15–18
  - [68] O’Connell J S and Schroder B 1988 *Phys. Rev.* **C38** 2447–2449
  - [69] Ankowski A M, Benhar O and Sakuda M 2015 *Phys. Rev.* **D91** 033005 (Preprint 1404.5687)
  - [70] De Pace A, Nardi M, Alberico W M, Donnelly T W and Molinari A 2003 *Nucl. Phys.* **A726** 303–326 (Preprint nucl-th/0304084)
  - [71] Delorme J and Ericson M 1985 *Phys.Lett.* **B156** 263
  - [72] Marteau J, Delorme J and Ericson M 2000 *Nucl.Instrum.Meth.* **A451** 76–80
  - [73] Aguilar-Arevalo A A *et al.* (MiniBooNE) 2010 *Phys. Rev.* **D81** 092005 (Preprint 1002.2680)
  - [74] Martini M, Ericson M, Chanfray G and Marteau J 2009 *Phys.Rev.C* **80** 065501 (Preprint 0910.2622)
  - [75] Martini M, Ericson M, Chanfray G and Marteau J 2010 *Phys.Rev.C* **81** 045502 (Preprint 1002.4538)
  - [76] Martini M, Ericson M and Chanfray G 2011 *Phys.Rev.* **C84** 055502 (Preprint 1110.0221)
  - [77] Nieves J, Ruiz Simo I and Vicente Vacas M 2011 *Phys.Rev.C* **83** 045501 (Preprint 1102.2777)
  - [78] Lalakulich O, Gallmeister K and Mosel U 2012 *Phys.Rev.* **C86** 014614 (Preprint 1203.2935)
  - [79] Rodrigues P A *et al.* (MINERvA) 2016 *Phys. Rev. Lett.* **116** 071802 [Addendum: *Phys. Rev. Lett.*121,no.20,209902(2018)] (Preprint 1511.05944)
  - [80] Ruiz Simo I, Albertus C, Amaro J, Barbaro M, Caballero J *et al.* 2014 *Phys.Rev.* **D90** 033012 (Preprint 1405.4280)
  - [81] Megias G, Donnelly T, Moreno O, Williamson C, Caballero J *et al.* 2015 *Phys.Rev.* **D91** 073004 (Preprint 1412.1822)
  - [82] Megias G D, Amaro J E, Barbaro M B, Caballero J A and Donnelly T W 2016 *Phys. Rev.* **D94** 013012 (Preprint 1603.08396)
  - [83] Megias G, Amaro J, Barbaro M B, Caballero J A, Donnelly T W and Ruiz Simo I 2016 *Phys. Rev.* **D94** 093004 (Preprint 1607.08565)
  - [84] Ruiz Simo I, Amaro J E, Barbaro M B, De Pace A, Caballero J A, Megias G D and Donnelly T W 2016 *Phys. Lett.* **B762** 124–130 (Preprint 1607.08451)
  - [85] Duer M *et al.* (CLAS) 2018 (Preprint 1810.05343)
  - [86] Ruiz Simo I, Amaro J E, Barbaro M B, De Pace A, Caballero J A, Megias G D and Donnelly T W 2016 *Phys. Rev.* **C94** 054610 (Preprint 1606.06480)
  - [87] Bosted P E and Mamyan V 2012 (Preprint 1203.2262)
  - [88] Christy E 2015 private communication
  - [89] Walecka D 1975 *Muon Physics, Sect. 4* (Academic Press)
  - [90] O’Connell J S, Donnelly T W and Walecka J D 1972 *Phys. Rev.* **C6** 719–733
  - [91] Marteau J 1999 *Eur.Phys.J.A* **5** 183–190 (Preprint hep-ph/9902210)
  - [92] Dolan S, Mosel U, Gallmeister K, Pickering L and Bolognesi S 2018 *Phys. Rev.* **C98** 045502 (Preprint 1804.09488)
  - [93] Pinzon Guerra E S *et al.* 2019 *Phys. Rev.* **D99** 052007 (Preprint 1812.06912)
  - [94] Stowell P *et al.* (MINERvA) 2019 (Preprint 1903.01558)
  - [95] Rein D and Sehgal L M 1981 *Annals Phys.* **133** 79–153
  - [96] Graczyk K M and Sobczyk J T 2008 *Phys. Rev.* **D77** 053001 (Preprint 0707.3561)
  - [97] Leitner T, Buss O, Mosel U and Alvarez-Ruso L 2008 *PoS NUFAC08* 009 (Preprint 0809.3986)
  - [98] Golan T, Juszczak C and Sobczyk J T 2012 *Phys.Rev.* **C86** 015505 (Preprint 1202.4197)
  - [99] Leitner T J 2009 *Neutrino-nucleus interactions in a coupled-channel hadronic transport model* dissertation Giessen University Germany <http://www.uni-giessen.de/diss/leitner/2009>
  - [100] Drechsel D, Kamalov S S and Tiator L 2007 *Eur. Phys. J. A* **34** 69–97 (Preprint 0710.0306)
  - [101] Leitner T, Alvarez-Ruso L and Mosel U 2006 *Phys. Rev.* **C73** 065502 (Preprint nucl-th/

- 0601103)
- [102] Albright C H and Liu L S 1965 *Phys. Rev.* **140** B748–B761
  - [103] Lalakulich O and Paschos E A 2005 *Phys. Rev.* **D71** 074003 (*Preprint hep-ph/0501109*)
  - [104] Adler S L 1968 *Annals Phys.* **50** 189–311
  - [105] Leitner T, Alvarez-Ruso L and Mosel U 2006 *Phys. Rev.* **C74** 065502 (*Preprint nucl-th/0606058*)
  - [106] Hernandez E, Nieves J, Valverde M and Vicente Vacas M J 2010 *Phys. Rev.* **D81** 085046 (*Preprint 1001.4416*)
  - [107] Lalakulich O, Leitner T, Buss O and Mosel U 2010 *Phys. Rev.* **D82** 093001 (*Preprint 1007.0925*)
  - [108] Wilkinson C, Rodrigues P, Cartwright S, Thompson L and McFarland K 2014 *Phys. Rev.* **D90** 112017 (*Preprint 1411.4482*)
  - [109] Wu J J, Sato T and Lee T S H 2015 *Phys. Rev.* **C91** 035203 (*Preprint 1412.2415*)
  - [110] Krusche B, Lehr J, Ahrens J, Annand J, Beck R *et al.* 2004 *Eur. Phys. J.* **A22** 277–291 (*Preprint nucl-ex/0406002*)
  - [111] Krusche B, Lehr J, Bloch F, Kotulla M, Metag V, Mosel U and Schadmand S 2004 *Eur. Phys. J.* **A22** 347–351 (*Preprint nucl-ex/0411009*)
  - [112] Clasie B *et al.* 2007 *Phys. Rev. Lett.* **99** 242502 (*Preprint 0707.1481*)
  - [113] El Fassi L *et al.* (CLAS) 2012 *Phys. Lett.* **B712** 326–330 (*Preprint 1201.2735*)
  - [114] Hernandez E, Nieves J and Valverde M 2007 *Phys. Rev.* **D76** 033005 (*Preprint hep-ph/0701149*)
  - [115] Alvarez-Ruso L, Hernández E, Nieves J and Vacas M J V 2016 *Phys. Rev.* **D93** 014016 (*Preprint 1510.06266*)
  - [116] Nakamura S X, Kamano H and Sato T 2015 *Phys. Rev.* **D92** 074024 (*Preprint 1506.03403*)
  - [117] Salcedo L L, Oset E, Vicente-Vacas M J and Garcia-Recio C 1988 *Nucl. Phys.* **A484** 557–592
  - [118] Leader E and Predazzi E 1996 *An introduction to gauge theories and modern particle physics* (Cambridge: Cambridge University Press)
  - [119] Sjostrand T, Mrenna S and Skands P Z 2006 *JHEP* **05** 026 (*Preprint hep-ph/0603175*)
  - [120] Lalakulich O, Gallmeister K and Mosel U 2012 *Phys. Rev.* **C86** 014607 (*Preprint 1205.1061*)
  - [121] Airapetian A *et al.* (HERMES) 2007 *Nucl. Phys.* **B780** 1–27 (*Preprint 0704.3270*)
  - [122] Lehmann I (HERMES) 2011 Hadronization in Nuclei - Multidimensional Study *Proceedings, 14th International Conference on Hadron spectroscopy (Hadron 2011): Munich, Germany, June 13-17, 2011* (*Preprint 1111.2522*) URL <http://www.slac.stanford.edu/econf/C110613/contributions/112-hadron2011.pdf>
  - [123] Accardi A, Arleo F, Brooks W K, D’Enterria D and Muccifora V 2010 *Riv. Nuovo Cim.* **32** 439–553 (*Preprint 0907.3534*)
  - [124] Gallmeister K and Mosel U 2008 *Nucl. Phys.* **A801** 68–79 (*Preprint nucl-th/0701064*)
  - [125] <http://www.fluka.org/fluka.php>
  - [126] Ruterbories D *et al.* (MINERvA) 2019 *Phys. Rev.* **D99** 012004 (*Preprint 1811.02774*)
  - [127] Mosel U and Gallmeister K 2019 *Phys. Rev.* **C99** 035502 (*Preprint 1708.04528*)
  - [128] Ankowski A and Friedland A 2019, to be published
  - [129] Ashkenazi A private communication, June 2018
  - [130] Zmuda J, Graczyk K M, Juszczak C and Sobczyk J T 2015 NuWro Monte Carlo generator of neutrino interactions - first electron scattering results *Matter To The Deepest, Recent Developments In Physics Of Fundamental Interactions Ustron, Poland, September 13-18, 2015* (*Preprint 1510.03268*) URL <http://inspirehep.net/record/1397207/files/arXiv:1510.03268.pdf>
  - [131] Effenberger M, Hombach A, Teis S and Mosel U 1997 *Nucl. Phys.* **A614** 501–520 (*Preprint nucl-th/9610022*)
  - [132] Lehr J, Effenberger M and Mosel U 2000 *Nucl. Phys.* **A671** 503–531 (*Preprint nucl-th/9907091*)
  - [133] Lehr J and Mosel U 2002 *Nucl. Phys.* **A699** 324–327 (*Preprint nucl-th/0108018*)
  - [134] Lehr J and Mosel U 2003 *Phys. Rev.* **C68** 044603 (*Preprint nucl-th/0307009*)
  - [135] Lehr J, Post M and Mosel U 2003 *Phys. Rev.* **C68** 044601 (*Preprint nucl-th/0306024*)

- [136] Buss O, Alvarez-Ruso L, Muhlich P and Mosel U 2006 *Eur.Phys.J.* **A29** 189–207 (*Preprint nucl-th/0603003*)
- [137] Buss O, Alvarez-Ruso L, Larionov A B and Mosel U 2006 *Phys. Rev. C* **74** 044610 (*Preprint nucl-th/0607016*)
- [138] Buss O, Leitner T, Mosel U and Alvarez-Ruso L 2007 *Phys.Rev.* **C76** 035502 (*Preprint 0707.0232*)
- [139] Buss O, Leitner T, Mosel U and Alvarez-Ruso L 2008 (*Preprint 0809.2550*)
- [140] Gallmeister K, Kaskulov M and Mosel U 2011 *Phys. Rev.* **C83** 015201 (*Preprint 1007.1141*)
- [141] Hombach A, Engel A, Teis S and Mosel U 1995 *Z.Phys.* **A352** 223–230 (*Preprint nucl-th/9411025*)
- [142] Muhlich P, Falter T and Mosel U 2004 *Eur. Phys. J.* **A20** 499–508 (*Preprint nucl-th/0310067*)
- [143] Muhlich P, Falter T, Greiner C, Lehr J, Post M and Mosel U 2003 *Phys. Rev.* **C67** 024605 (*Preprint nucl-th/0210079*)
- [144] Kaskulov M M, Gallmeister K and Mosel U 2009 *Phys. Rev.* **C79** 015207 (*Preprint 0808.2564*)
- [145] Kaskulov M M and Mosel U 2011 *Phys.Rev.* **C84** 065206 (*Preprint 1103.2097*)
- [146] Acciarri R *et al.* (ArgoNeuT Collaboration) 2014 *Phys.Rev.Lett.* **113** 261801 (*Preprint 1408.0598*)
- [147] <http://home.fnal.gov/~ljf26/DUNEFluxes/>
- [148] Abbott D *et al.* 1998 *Phys. Rev. Lett.* **80** 5072–5076
- [149] Garrow K *et al.* 2002 *Phys. Rev.* **C66** 044613 (*Preprint hep-ex/0109027*)
- [150] O'Neill T G *et al.* 1995 *Phys. Lett.* **B351** 87–92 (*Preprint hep-ph/9408260*)
- [151] Lehr J 2003 *In-Medium Eigenschaften von Nukleonen und Nukleonresonanzen in einem semiklassischen Transportmodell* Ph.D. thesis Giessen University Germany available online at <http://www.uni-giessen.de/fbz/fb07/fachgebiete/physik/institute/theorie/inst/theses/dissertation/previous>
- [152] Acciarri R *et al.* (DUNE) 2015 (*Preprint 1512.06148*)
- [153] Andreopoulos C *et al.* 2018 <https://genie-docdb.pp.rl.ac.uk/cgi-bin/ShowDocument?docid=2>
- [154] Mertens T *et al.* (CBELSA) 2008 *Eur. Phys. J.* **A38** 195–207 (*Preprint 0810.2678*)
- [155] Nanova M *et al.* (CBELSA/TAPS) 2010 *Phys. Rev.* **C82** 035209 (*Preprint 1005.5694*)
- [156] Alvarez-Ruso L *et al.* 2018 *Prog. Part. Nucl. Phys.* **100** 1–68 (*Preprint 1706.03621*)
- [157] Cassing W 2009 *Eur. Phys. J. ST* **168** 3–87 (*Preprint 0808.0715*)